UNIVERSIDADE DO VALE DO RIO DOS SINOS
Programa de Pós-Graduação em Geologia
Área de Concentração em Geologia Sedimentar
Linha de Pesquisa em Sensoriamento Remoto e Modelagem Geológica

DISSERTAÇÃO DE MESTRADO

A COMPARTIMENTAÇÃO HIDROGEOLÓGICA DO SISTEMA AQUÍFERO SERRA GERAL (SASG) E SISTEMA AQUÍFERO GUARANI (SAG): UM ESTUDO NA REGIÃO DA ESCARPA BASÁLTICA NORDESTE DO RIO GRANDE DO SUL

Rafaela Christ da Silva

Orientador: Dr. Francisco M. Wohnrath Tognoli (PPGEO UNISINOS)
Coorientador: Dr. Pedro A. Roehe Reginato (IPH-UFRGS)

São Leopoldo/RS, julho/2019.

S586c Silva, Rafaela Christ da.

A compartimentação hidrogeológica do Sistema Aquífero Serra Geral (SASG) e Sistema Aquífero Guarani (SAG) : um estudo na região da escarpa basáltica nordeste do Rio Grande do Sul / Rafaela Christ da Silva. – 2019.

66 f. : il. ; 30 cm.

Dissertação (mestrado) – Universidade do Vale do Rio dos Sinos, Programa de Pós-Graduação em Geologia, 2019.

"Orientador: Dr. Francisco M. Wohnrath Tognoli (PPGEO UNISINOS) Coorientador: Dr. Pedro A. Roehe Reginato (IPH-UFRGS)."

1. Fluxo subterrâneo. 2. Conexão fraturado-granular. 3. Paraná, Rio, Bacia. 4. Compartimentalização tectônica. 5. Lineamentos. I. Título.

(Bibliotecária: Amanda Schuster – CRB 10/2517)

Rafaela Christ da Silva

A COMPARTIMENTAÇÃO HIDROGEOLÓGICA DO SISTEMA AQUÍFERO SERRA GERAL (SASG) E SISTEMA AQUÍFERO GUARANI (SAG): UM ESTUDO NA REGIÃO DA ESCARPA BASÁLTICA NORDESTE DO RIO GRANDE DO SUL

Dissertação de Mestrado apresentada como parte das exigências para a obtenção do título de Mestre, pelo Programa de Pós-Gradução em Geologia da Universidade do Vale do Rio dos Sinos (UNISINOS).

Área de Concentração: Geologia Sedimentar
Linha de Pesquisa: Sensoriamento Remoto e Modelagem Geológica

Orientador: Dr. Francisco M. Wohnrath Tognoli (PPGEO UNISINOS)
Coorientador: Dr. Pedro A. Roehe Reginato (IPH-UFRGS)

São Leopoldo/RS, julho/2019.

Desafios: onde a magia da vida acontece.

(Autor desconhecido, paredes de um bar)

AGRADECIMENTOS

As nossas escolhas definem quem nos tornamos. Escolher estudar e ser geologia, sem dúvidas, trouxe à tona a melhor parte de mim e foi o caminho que me levou a descobrir a minha essência.

Agradeço imensamente a todos os envolvidos nesta pesquisa: a PROSUC/CAPES pela concessão da bolsa de estudo; ao Projeto VizGEO, pelo suporte financeiro dos campos e análises; ao LASERCA/UNISINOS pelos *softwares* e materiais disponibilizados; ao IPH/UFRGS, pelo espaço no seu programa de pós graduação e pela possibilidade da realização das disciplinas; ao professor Paulo Salvadoretti, ao doutorando Geroge Olufunmilayo Gasper e ao PPGEM/UFGRS pela ajuda no campo e na utilização do equipamento de perfilagem ótica (OTV) e posteriormente, na compilação dos dados e disponibilização do *software* WellCad; ao Lauro Moreira da Rosa e ao Adriano Baz Pereira, do Laboratório de Laminação da UNISINOS, pela confecção das lâminas; ao graduando Maurício Righi pela ajuda com a contagem de pontos e interpretação das lâminas. Ao SIAGAS/CPRM, CORSAN, SEHASB e HIDROGEO pela disponibilidade dos dados de poços.

Ao meu orientador, Francisco Tognoli, que me acompanha desde o dia que eu decidi cursar geologia e que me ajudou tantas vezes a manter a calma no meio do tumulto da pesquisa. Ao meu coorientador Pedro Reginato, que me recebeu de braços abertos desde o início. Vocês são pessoas e professores incríveis, pacientes e de um coração enorme. Obrigada por todo o conhecimento que compartilharam comigo e pela amizade que criamos.

Ao meu namorado, Itallo, que além de me ajudar em todas as partes que envolveram habilidades de desenho na minha pesquisa, me auxiliou em campo, em discussões, e de tantas formas que eu não conseguiria lembrar. Obrigada por ter sido o meu porto seguro ao longo desta jornada.

À minha família: todas minhas conquistas são dedicadas a vocês. Aos meus pais, Felipe e Cristiane, que mesmo sem perceberem, me ensinaram a alçar voos altos e a acreditar que com muita dedicação e coragem, nada é impossível. A minha irmã, Júlia, minha parte doce e melhor amiga em todos os momentos. Ao meu tio e dindo, Marcelo, a pessoa que me desafia e me acalma, por todo o apoio nessa vida geológica que, com muito prazer, nós temos a oportunidade de compartilhar. Aos meus avós, Marino e Cita (*in memorian*) e Tonho e Clarí, por me permitirem crescer e aprender ao seu lado e por sempre encherem o meu coração com um amor inigualável.

Aos meus colegas e amigos da Geoambiental, por serem tão compreensivos, amigos e parceiros todas as vezes que eu precisei me dedicar mais a minha pesquisa do que ao trabalho. A Cristiane, Jéssica e Gustavo, pela nossa amizade que me traz paz. A Laís, pela companhia e amizade que se fortaleceu nesta etapa, além dos inúmeros auxílios geológicos. A toda equipe do VizGEO e aos amigos da geologia, pela parceria com a sala de estudos e pela convivência que deixou mais uma vez, a caminhada bem mais leve.

E por fim, ao meu professor e orientador da graduação, Osmar Coelho, que foi quem me introduziu a este mundo da hidrogeologia.

SUMÁRIO

LISTA DE FIGURAS

LISTA DE FIGURAS DO ARTIGO

LISTA DE TABELAS DO ARTIGO

RESUMO

A área de estudo, situada na porção sul da Bacia do Paraná, no nordeste do Estado do Rio Grande do Sul, Brasil, possui como fontes de abastecimento dois importantes sistemas aquíferos, o Guarani (SAG) e o Serra Geral (SASG). O primeiro, constituído pela porosidade secundária nas rochas vulcânicas da Formação Serra Geral e o segundo, pela porosidade primária nos arenitos da Formação Botucatu. Por abranger uma zona de contato litológico, as estruturas tectônicas que interceptam as pilhas de derrames vulcânicos podem afetar as rochas areníticas do SAG e dependendo de suas características como orientação e tipo de fraturamento, proporcionar a conexão entre os dois aquíferos, afetar diretamente a sua produtividade, e promover a compartimentação hidrogeológica. Para o presente estudo foram utilizados dados de 375 poços que captam água subterrânea do SASG, do SAG e de ambos os sistemas, a fim de avaliar as características hidrodinâmicas, de potenciometria e altimetria do contato litológico. Estes dados foram analisados juntamente com lineamentos estruturais regionais, medidas de juntas em mais de 100 afloramentos de rochas vulcânicas e areníticas e análises petrográficas para avaliação da porosidade e tipos de cimento. Os resultados demonstraram a ocorrência de compartimentos hidrogeológicos distintos controlados por zonas de falha de orientação NW,NNW, and NNE, conexão por juntas e, localmente, falhas. As características texturais e composicionais dos arenitos controlam a preservação ou obliteração do sistema poroso e determinam seu comportamento produtivo como aquífero. A superfície do contato entre as formações Botucatu e Serra Geral é favorável à circulação e armazenamento de água subterrânea conforme corroborado por 93% dos poços que atravessaram essa superfície. A integração dos resultados permitiu propor um modelo hidrogeológico conceitual integrando os sistemas aquíferos Guarani e Serra Geral.

Palavras-chave: Fluxo subterrâneo, Conexão fraturado-granular, Lineamentos, Compartimentalização tectônica, Bacia do Paraná.

1. APRESENTAÇÃO

Atualmente o uso da água subterrânea para fins de abastecimento urbano e industrial é significativo e mostra uma nítida tendência de crescimento. O seu custo de produção, quando comparado aos recursos hídricos superficiais, é efetivamente mais baixo, uma vez que necessita de menor infraestrutura e tratamento (Foster, *et al*., 1993; Rebouças, *et al*., 2006). Por este motivo, muitos estudos vêm sendo desenvolvidos visando a compreensão do fluxo subterrâneo em sistemas aquíferos, tanto granulares, formados pela porosidade primária nas rochas sedimentares, como fraturados, pela porosidade secundária nas rochas ígneas, metamórficas e sedimentares muito litificadas (Machado, 2005).

A área de estudo, situada na região nordeste da Escarpa Basáltica no Rio Grande do Sul, é constituída pelas rochas vulcânicas da Formação Serra Geral que formam o Sistema Aquífero Serra Geral (SASG), fraturado e pelas rochas sedimentares da Formação Botucatu e Pirambóia, que fazem parte do Sistema Aquífero Guarani (SAG), granular.

Segundo Machado (2005) a atual estruturação do SAG, no Estado, está condicionada aos eventos tectônicos que afetaram os domínios geológicos do escudo pré-cambriano aos derrames vulcânicos, bem como as sucessivas reativações que ocorreram principalmente do final do Permiano até o Cretáceo (Giardin & Faccini, 2002).

Neste contexto, as regiões de fraqueza litosférica e crustal, oriundas da fragmentação do Supercontinente Gondwana e posterior formação do Oceano Atlântico, que resultaram no extravasamento vulcânico da Formação Serra Geral, afetaram diretamente as rochas sotopostas da Formação Botucatu. As estruturas tectônicas que interceptam os pacotes vulcânicos podem afetar os arenitos e proporcionar, dependendo de suas características físicas, em determinados locais, a formação de compartimentos hidrogeológicos, bem como a conexão entre os dois aquíferos.

Há evidências da existência de recarga vertical do SAG através de fraturas tectônicas que cortam os basaltos da Formação Serra Geral, na região de Ribeirão Preto e São Paulo (Fernandes *et al*.; 2011; Fernandes *et al*.; 2012; Fernandes *et al*., 2016). Além disso, segundo Araújo *et al*. (1995), Machado (2005), Heine (2008) e Matos *et al*. (2018) a geometria do SAG, no Rio Grande do Sul, é controlada por fatores tectônico-estruturais, sendo que Heine (2008) e Matos *et al*. (2018) apontam que a recarga do SAG pode ocorrer por meio das fraturas oriundas dos derrames vulcânicos.

O objetivo deste estudo é identificar, por meio de características estruturais, hidrogeológicas e litológicas, a possível existência de uma compartimentação, controlada principalmente pelo arcabouço geotectônico e consequentemente geomorfológico, a fim de compreender a conexão entre o sistema aquífero fraturado (SASG) e granular (SAG) e os fatores que influenciam a sua produtividade.

Esta pesquisa foi estruturada em duas partes. A primeira, apresentará uma breve revisão bibliográfica acerca do tema estudado e a segunda, os resultados obtidos, que foram compilados junto ao artigo submetido ao periódico *Hydrogeology Journal*.

2. PARTE I: CONTEXTUALIZAÇÃO:

2.1 Estruturas Tectônicas Rúpteis

O estudo das estruturas geométricas, cinemáticas e dos sucessivos eventos de sua formação e modificação, permite relacionar os episódios a arranjos pretéritos e atuais, visando entender o campo de tensões específico que agiu sobre um determinado corpo rochoso (Almeida & Hasui, 1984; Sibson, 1994).

As análises geométricas, cinemáticas e dinâmicas são realizadas para compreender os eventos geotectônicos e a formação das descontinuidades, conhecidas como estruturas primárias e secundárias (Chiang, 1984, Hausman, 1995; Reginato, 2003). As primárias são definidas como aquelas constituídas durante a formação das rochas, como as estratificações em rochas sedimentares e diacláses e zonas vesiculares amígdaloidais em rochas vulcânicas cuja interpretação principal se detém à determinação do topo e da base de uma sequência, como os fluxos de lava, estratificações e vesículas amígdaloidais. As secundárias são formadas em rochas ígneas e sedimentares após a sua consolidação e, em metamórficas, durante e após o seu processo de gênese, caracterizadas por juntas, fraturas de cisalhamento, dobras, clivagens, foliações, lineações e *shear zones*.

Embora seja difícil estimar com precisão os valores absolutos de um campo de tensões, as análises de famílias de estruturas rúpteis, como falhas, fraturas e juntas permitem a reconstrução das paleotensões tectônicas, uma vez que as interpretações estruturais destes sistemas se baseiam na relação entre os planos de falhas com suas estrias, sentido de movimento e elipsóide de tensão (Coriolano, *et al*., 1997; Menezes & Jardim de Sá, 1999; Fernandes & Rudolph, 2011). Desta forma, obtém-se as orientações de paleostress, utilizando a união dos dados de direção e mergulho do plano de falha, orientação da lineação e sentido do movimento.

Em estudos abordando sistemas aquífero fraturados, estes conhecimentos são necessários, uma vez que o armazenamento e permeabilidade da água subterrânea são relacionados às tensões atuantes nas estruturas secundárias, fraturas, juntas e falhas que são favoráveis a estes processos (Feitosa & Manoel, 2000).

2.2 Neotectônica

Embora existam muitos estudos que enfatizem o levantamento e as análises de estruturas tectônicas rúpteis que afetam as sucessões cenozoicas, com a definição de sequências de eventos tectônicos responsáveis pela formação e deformação de cada área estudada para o entendimento de eventos geológicos ou morfotectônicos (Riccomini; 1989; Saadi, 1993; Salvador;1994; Salvador e Riccomini, 1995; Albuquerque, 2004; Silva, 2006 e Bricalli, 2011) ainda há várias divergências deste termo, de acordo com a concepção de distintos autores. Para alguns, este tipo de estudo está relacionado apenas à um aspecto temporal, enquanto que, para outros, além disso, o mesmo também é correlacionado a modelagem da topografia contemporânea.

O termo Neotectônica foi introduzido por Obruchev (1948), para designar eventos tectônicos com ocorrência durante o período Terciário ao Quaternário (Saadi, 1993), que subdividiu os mesmos em três tipos: a) movimentos alpinos, ocorridos do Cretáceo até hoje; b) movimentos recentes, do Plioceno ao recente; que correspondem aos movimentos neotectônicos propriamente dito e; c) movimentos modernos, os atuais.

Stewart e Hancock (1994) afirmam que a neotectônica estabelece um ramo da tectônica ligada ao estudo dos movimentos que ocorreram no passado e continuam ocorrendo no presente e que as estruturas neotectônicas estariam relacionadas ao regime tectônico atual e antigo, tendo sido geradas ou reativadas em um campo de esforços e deformação. Enquanto isso, Hasui (1990) define que os eventos neotectônicos estão relacionados diretamente à tectônica ressurgente e que durante a atuação de um regime de esforços, dependendo da orientação da falha pré-existente, em relação aos esforços tectônicos e a intensidade destes, é mais fácil reativar o campo de *stress* da mesma do que criar uma nova estrutura.

Segundo Hausui (1990), no território brasileiro, os eventos neotectônicos estariam relacionados ao processo de deriva da placa Sul-Americana e consequentemente, à migração do continente sul-americano e abertura do Atlântico Sul, iniciada no Cenozoico Médio, considerando que essas movimentações ocorrem até os dias atuais. Como o Brasil está localizado nesta zona de margem passiva, os esforços tectônicos ocorrem em função, essencialmente, da interação de dois processos: forças de empurrão, exercidas principalmente pela abertura da Cordilheira Meso-Atlântica (*ridge push*) e esforços compressionais, transmitidos a partir do limite oeste da placa, na fossa Peru - Chile (Coblentz e Richardson, 1996). Em nível regional, além do empurrão da cordilheira, deve-se considerar também o movimento decorrente da subducção da Placa de Nazca (*slab pull*) e, em nível local, as forças associadas às margens continentais e às áreas elevadas (Coblentz e Richardson, 1996).

Saadi (1993) expõe que a plataforma brasileira teria sido afetada por deformações tectônicas cenozóicas em toda sua extensão e, que estas, seguiram preferencialmente os locais de antigas linhas de fraqueza crustal, ocorridas em deformações pretérita, podendo, a partir destas estruturas, ter originado novos planos de fraqueza. Para este autor, as principais descontinuidades crustais reativadas limitam uma compartimentação do território brasileiro segundo as atividades neotectônicas, sendo que as tensões atuais estariam convergindo em torno de um vetor compressivo horizontal de direção NW – SE, com algumas variações E – W e N – S, provavelmente relacionadas às tensões residuais locais.

A partir destes conceitos, os estudos envolvendo a neotectônica e a análise destas feições, podem ser aplicados em distintas linhas de pesquisa, como por exemplo, a hidrogeologia em meios fraturados. A relação destes esforços contemporâneos permite avaliar a permeabilidade das fraturas e inferir sobre o fluxo de fluídos, tanto superficial, quanto subterrâneo (Stewart & Hancock, 1994; Aydin, 2000, Fernandes e Rudolph, 2001). Para determinação destas estruturas recentes, realiza-se a análise geomorfológica, na qual se admite que tais aspectos tenham sido causados por movimentações tectônicas, admitindo-se que as diferenças no relevo foram originadas a partir do controle tectônico ativo

(Summerfield, 1986). Desta forma, a morfotectônica se afixa nas feições geomorfológicas resultantes das tensões neotectônicas, pois as mesmas, derivadas de ação tectônica antiga, apresentam modificações das características de seus tensores de *stress*, devido à erosão sofrida no decorrer do tempo geológico (Bloom, 1991), não sendo mais possível identificar com clareza a influência tectônica em sua gênese; além de proporcionar feições singulares em margens passivas, de modo que sejam identificadas com características próprias de morfologias que sofreram controle neotectônico (Burbank e Anderson, 2001).

As *landforms* ou então paisagens do relevo expressam diversos destes espectros de feições topográficas que podem ser analisados a fim de investigar o tipo, a magnitude e a recorrência dos movimentos tectônicos atuantes em determinado local (Stewart & Hancock, 1994). Desta forma, as falhas antigamente ativas, originam estruturas variadas, que irão refletir na compartimentação geomorfológica, sendo que, para cada qual, irá criar-se um padrão específico (Summerfield, 1986). As falhas normais podem gerar feições morfotectônicas do tipo escarpas, que podem apresentar *fronts* lineares ou escalonados, facetas trapezoidais e triangulares, e *horst* e grábens. Falhas transcorrentes podem gerar as seguintes feições morfotectônicas de escarpas, vales lineares, *sag ponds*, cristas lineares de *pressure ridges* e *shutter ridge*. E, as falhas reversas, podem gerar escarpas, colinas anticlinais (*upwarps*) e colinas sinclinais (*downwarps*) (Summerfield, 1986). Todas feições morfotectônicas citadas são comuns no sudeste do Brasil (Bricalli, 2011), destacando-se ainda a existência de algumas outras não comentadas acima.

Para caracterizar a compartimentação morfotectônica, realiza-se a análise de lineamentos utilizando imagens de satélite. Os lineamentos morfoestruturais caracterizam-se por arquivos vetoriais derivados da análise visual de imagens do relevo sombreado, a partir do qual pode-se obter os cálculos dos azimutes correspondentes a cada uma das destas linhas, ou seja, o seu sentido direcional (Feitosa, *et al.*, 2008). Segundo O'Leary (1976) são mapeados a partir de características lineares simples ou compostas de uma superfície e, cujas partes estão alinhadas em uma relação retilínea ou ligeiramente curvilínea, que difere distintamente dos padrões adjacentes. Podem estar associados a estruturas de subsuperfície, especialmente, as linhas de fraqueza pré-cambrianas, sendo que, as reativações destas estruturas têm sido documentadas como aspecto fundamental para o entendimento das manifestações neotectônicas no Brasil (Hasui, 1990; Saadi, 1993; Bricalli, 2011).

Strieder & Amaro (1997) distinguem os lineamentos em dois tipos: o tipo 1, associados a estruturas regionais representadas pela erosão de feições estrururais coesivas associadas ao tipo de litológica, havendo possibilidade de serem considerados como lineamentos compostos. Em pequenas escalas, tendem a modelar as formas estruturais; tipo 2: associados a estruturas rúpteis e expressos por feições geomorfológicas negativas, geralmente truncando os limites litológicos (falhas ou juntas). São geralmente retilíneos e representados por drenagens controlados por fraturas, que possuem distribuição espacial, orientação azimutal e comprimentos bem definidos (Reginato, 2003).

2.3 Aquíferos em Domínios Fraturados

Aquíferos são considerados unidades geológicas permeáveis e saturadas que exercem a capacidade de armazenar e transmitir significativas quantidades de água (Freeze & Cherry, 1979). Existem alguns parâmetros hidrogeológicos fundamentais para definição do fluxo subterrâneo e caracterização dos diferentes tipos de aquíferos, como as características hidráulicas destes meios, representadas pela porosidade, condutividade hidráulica, transmissividade e coeficiente de armazenamento (Machado, 2005). Neste estudo, será abordado especialmente os conceitos de porosidade e permeabilidade.

As rochas fraturadas são geralmente heterogêneas e anisotrópicas, porém, o seu meio fraturado pode ser contínuo ou descontínuo. Se o fraturamento for muito intenso, a ponto do meio se comportar hidraulicamente como poroso, é possível considerá-lo como um "contínuo equivalente" e determinar suas características hidráulicas (Freeze e Cherry, 1979).

No meio contínuo utiliza-se a Lei de Darcy (utilizada para meios heterogêneos, quando equivalentes a meios homogêneios), onde é possível aplicar a Lei Cúbica, (Snow, 1969).

$$K = \frac{\rho g \times Nb^3}{12\mu}$$

Onde,

K = condutividade hidráulica;

ρ = densidade da água;

μ = viscosidade da água;

g = aceleração da gravidade;

N = número de fraturas por unidade de distância (frequência) e;

b = abertura das fraturas.

A Lei Cúbica demonstra que a condutividade hidráulica em meios fraturados é proporcional ao cubo da abertura da fratura. A frequência e a abertura das fraturas são bastante variadas, assim, mesmo quando o meio for homogêneo, irá se comportar como anisotrópico e, apresentar diferentes condutividades hidráulicas, em distintas direções. Se ocorrer uma rede de fraturas interconectadas é possível definir uma superfície potenciométrica, formada pelas intersecções do nível freático em cada fratura e por um plano horizontal imaginário (Custodio e Llamas, 1996).

A fim de definir as propriedades hidráulicas do meio fraturado como um meio contínuo utiliza-se o volume elementar representativo (VER) ou representative elementary volume (REV), que constitui o mínimo volume de rocha considerado representativo do meio fraturado (Figura 1). É comum a maior parte da água subterrânea de um poço tubular depender apenas de uma ou duas fraturas altamente produtivas e interconectadas com uma rede de fraturas alimentadoras menores, as quais mantém a produtividade (BANKS *et al*., 1996).

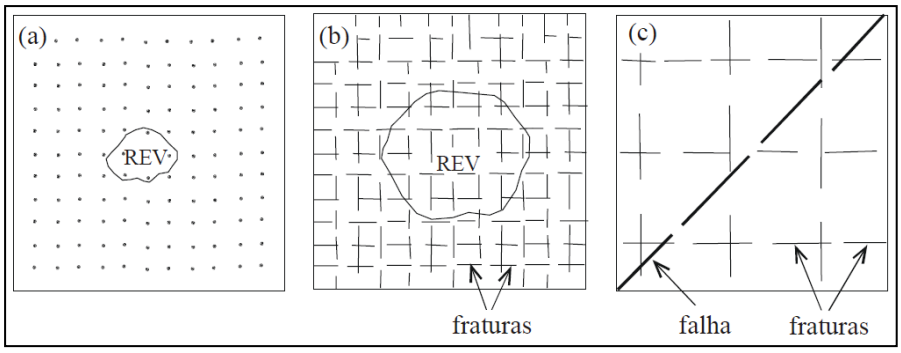

Figura 1: Volume Elementar Representativo (VER) em diferentes condições: (a) rocha porosa homogênea, (b) rocha fraturada homogênea e (c) rocha fraturada com grandes descontinuidades onde o VER é muito grande ou não existe. Fonte: Singhal E Gupta, 1999.

O comportamento hidráulico dos diferentes tipos de rochas constituintes de aquíferos fraturados é variável e depende das propriedades intrínsecas da rocha e, também de fatores externos, como o clima, o litotipo, a topografia, as formas de relevo e os fatores de intemperismo.

As descontinuidades são influenciadas pelo comportamento heterogêneo e anisotrópico dos aquíferos fraturados e podem ser agrupadas em três grupos: os planos de acamadamento que são as descontinuidades mais importantes das rochas, responsáveis pela anisotropia e fluxo da água; a foliação e a clivagem, que estão presentes nas rochas metamórficas, possuem alta influência no fluxo subterrâneo e podem ser equiparadas com o acamadamento nas rochas sedimentares; e, as fraturas, que são planos nos quais houve perda parcial ou total da coesão das rochas e se caracterizam como as descontinuidades mais importantes no controle do fluxo subterrâneo (Neves, 2005).

Segundo Banks *et al*. (1992) as fraturas e zonas de fraturas podem ser diferenciadas em três diferentes tipos: as fraturas individuais, que se formam em superfícies relativamente planas, sem formação de brechas; as zonas de brechas, que são caracterizadas por possuir mais de um conjunto de fraturas, com espaçamento reduzido, onde pode ocorrer formação de brecha, mas os planos de fraturas individuais ainda são reconhecíveis; e, as zonas de fraturas com alto grau de cominuição (crush zones), que são onde os planos de fraturas individuais não são possíveis de serem distinguidos e contêm tipicamente brecha de falha formada por clastos de tamanhos variados.

O arranjo das tensões que gerou as fraturas determina a sua abertura original (Figura 2). As fraturas de tração costumam ser mais produtivas do que as de cisalhamento, uma vez que estas últimas possuem uma menor abertura e são frequentemente preenchidas. A tensão é um fator que afeta a condutividade hidráulica de fraturas e do sistema de fraturas. A permeabilidade de uma rocha fraturada vai depender então, da tensão e, também da conexão desta rocha fraturada com um sistema de fraturas de diferentes orientações (Banks *et al*., 1996 e Odling, 1993). A influência do campo de tensões pode ser diminuída por outros fatores, como as propriedades das fraturas preexistentes, a sua orientação, conectividade, alteração e mineralização, mas, dependendo da área, a tensão pode ser um dos fatores determinantes na percolação do fluxo subterrâneo.

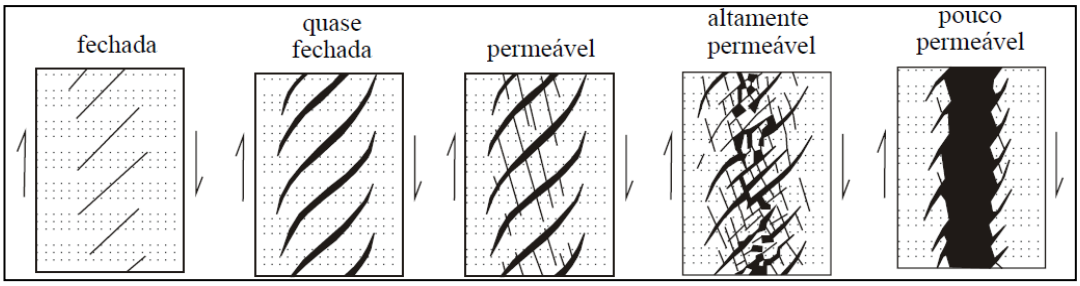

Figura 2: Estágios de desenvolvimento de uma zona de fraturas de cisalhamento e variação da permeabilidade. Fonte: Banks e Robins, 2002.

A rocha basáltica, devido à natureza do seu processo de formação, é extremamente heterogênea quanto às suas propriedades hidráulicas. O rápido resfriamento e o escape de gases geram estruturas de juntas e bolhas com espaços porosos, que resultam na alta permeabilidade e anisotropia (Freeze & Cherry, 1979), que dentro de um único fluxo podem exibir ótimas condutividades, vertical e horizontal. A permeabilidade horizontal está relacionada ao processo de gênese da rocha (Rebouças & Fraga, 1988) e a vertical, à sua estruturação tectônica. Esta última, permite que ocorra a percolação de água subterrânea com as estruturas interderrames (Rebouças & Fraga, 1988).

Quanto à sua estruturação, os derrames de rochas basálticas são constituídos por distintas zonas, os quais são caracterizados de acordo com as suas especificidades, como pode visualizar-se na Figura 3.

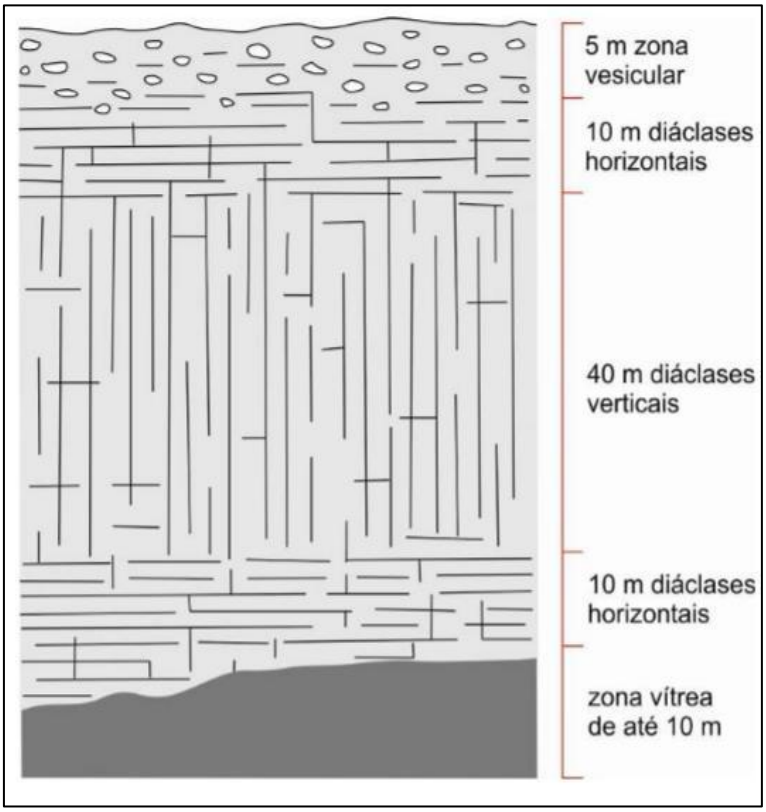

Figura 3: Modelo esquemático de um derrame basáltico em perfil. Fonte: Leinz (1949).

A zona vítrea, na porção inferior, é caracterizada por rocha basáltica vesicular e/ou amigdaloidal, com preenchimento de minerais secundários. Possuem estes horizontes de desgazeficação

devido ao rápido resfriamento da lava em contato com a superfície de fluxo (Guidicini & Campos 1968, Gomes 1996) e, quando intemperizada, a mesma pode apresentar-se como uma camada argilosa de alguns metros de espessura.

Acima, ocorre a zona de disjunção horizontal, caracterizada pelo diaclasamento em planos horizontais, espaçado em poucos centímetros, que condiciona a água subterrânea a uma circulação horizontal, geralmente não muito efetiva, devido à presença de materiais de alteração junto aos planos de fraturas. A zona seguinte, que compõe a porção central do derrame, é formada por rocha basáltica compacta com grau de cristalinidade variável, podendo atingir até 40,00 m de espessura (2/3 da espessura total em um derrame relativamente espesso) (Guidicini & Campos, 1968), e com predomínio de juntas (diacláses) verticais (Leinz, 1949). Nesta porção, o condicionamento geológico da rocha é desfavorável (Freeze & Cherry, 1979), uma vez que as mesmas são compartimentadas por intrusões (Rebouças & Fraga, 1988) ou por influxo de líquidos ao longo do tempo (Freeze & Cherry, 1979). Esta zona irá alimentar a seguinte, formada por diacláses horizontais subjacentes.

Em seguida, ocorre a zona de desgaseficação, constituída por um horizonte que tende a ser rico em vesículas e/ou amígdalas, que variam de milímetros até dezenas de centímetros, preenchidas por zeolitas, quartzo e calcedônica (podendo representar 30% a 40% do volume da rocha) (Gomes, 1996). Os gases da lava são aprisionados junto à superfície do derrame pelas placas já consolidadas em contato com a atmosfera, cuja mistura forma um complexo escoriáceo de aspecto esponjoso e de coloração avermelhada (Rebouças e Fraga, 1988). A permeabilidade desta porção depende da disposição espacial dos vacúolos (vesículas e/ou amígdalas), sendo que, quando os mesmos são interconectados por sistemas de faturamento, as condições de armazenamento de água subterrânea são excelentes (Rebouças e Fraga, 1988).

3. PARTE II: ARTIGO

Neste capítulo será apresentado o artigo submetido ao periódico *Hydrogeology Journal*,

Springer

Submission Confirmation

Thank you for your submission

Submitted to	Hydrogeology Journal
Manuscript ID	HJ-2019-6125
Title	HYDROGEOLOGICAL COMPARTMENTALIZATION AND CONNEXION OF THE GUARANI (GAS) AND SERRA GERAL (SGAS) AQUIFER SYST UNDER A MULTISCALAR PERSPECTIVE: A CASE STUDY IN SOUTHERN BRAZIL
Authors	Tognoli, Francisco Christ, Rafaela Reginato, Pedro Antonio Roehe Salvadoretti, Paulo
Date Submitted	11-Jul-2019

HYDROGEOLOGICAL COMPARTMENTALIZATION AND CONNEXION OF THE GUARANI (GAS) AND SERRA GERAL (SGAS) AQUIFER SYSTEMS UNDER A MULTISCALAR PERSPECTIVE: A CASE STUDY IN SOUTHERN BRAZIL

Rafaela Chirst[1]

Francisco Manoel Wohnrath Tognoli [1]

Pedro Antonio Roehe Reginatto [2]

Paulo Salvadoretti [3]

[1] Programa de Pós-Graduação em Geologia, Universidade do Vale do Rio dos Sinos (UNISINOS), Avenida Unisinos, 950, Cristo Rei, São Leopoldo, RS 93022.750, Brazil

[2] Instituto de Pesquisas Hidráulicas, Universidade Federal do Rio Grande do Sul, Avenida Bento Gonçalves, 9500, Agronomia, Porto Alegre, 91501-970, Brazil

[3] Programa de Pós-Graduação em Engenharia de Minas, Metalúrgica e de Materiais, Universidade Federal do Rio Grande do Sul, Avenida Bento Gonçalves, 9500, Agronomia, Porto Alegre, 91501-970, Brazil

Corresponding author: ftognoli@unisinos.br

ABSTRACT

Groundwater from the Guarani and Serra Geral aquifer systems are the principal source of water in Southern Brazil. The pore system is primary, intergranular, in the Guarani aquifer and secondary, associated with fractures in the Serra Geral aquifer. The investigation of the interrelationships of this dual-porosity is crucial to a better understanding of the compartmentalization and connexion, water storage, and productivity of both aquifers. Fault systems promoted the compartmentalization of the study area in six structural blocks. The contact between the aquifers presents high productivity, related to fractures present within each block. This study used data from 375 wells that produce groundwater from GAS, SGAS, or GAS+SGAS in order to evaluate hydrodynamic characteristics and elevation of the GAS-SGAS contact. The integration of data using remote sensing, structural data collected in more than 100 outcrops, and microscopic analysis of thin sections to estimate porosity and cement contents supported the interpretations of aspects of the compartmentalization and connexion of the aquifers. Fault zones of NW, NNW, and NNE orientation demarcate six structural blocks where the contact GAS-SGAS varies more than 400 m in elevation. Textural and compositional characteristics of sandstones analyzed in thin sections allowed understanding the relationship between types of porosity and content and types of cements. The surface that demarcates the contact Guarani-Serra Geral present high productivity in 93% of the wells drilled that reached both aquifers. The integration of the results allowed the proposition of a conceptual hydrogeological model for Guarani and Serra Geral aquifers in the study area.

Keywords: Goundwater flow, Granular-fractured connexion, Lineaments, Tectonic compartmentalization, Paraná Basin.

1. Introduction

Granular and fractured aquifer systems constitute the groundwater source responsible for the human, industrial, and agricultural activities throughout the world. Although granular aquifers have been used and studied since many decades ago, fractured aquifers have been a target of research in the last years and present many challenges in their understanding. Fractured aquifers have heterogeneous and anisotropic hydraulic properties (Lindholm and Vaccaro 1988; Reginato and Ahlert 2013) and groundwater storage and flow are controlled by fractures (Dafny *et al*. 2006) as well as by porous media such as amygdaloidal vesicle zones (Uhl and Joshi 1986). Both granular and fractured aquifers might occur in contact with one another, and hydraulic characteristics derived from their connexion and compartmentalization is not well known as well.

This context is particularly crucial for hydrogeological research once that Continental Flood Basaltic provinces (CFB) represent the most extensive magmatic flows recorded in the geological history (Jerram 2005) as recorded in the Deccan Plateau in India (Kulkarni *et al*. 2000; Katpatal *et al*. 2014), Paraná-Etendeka in South America and South Africa (Erlank *et al*. 1984; Peate 1990), Rio Columbia Plateau in USA (Whiteman *et al*. 1994), Golan Heights in Israel (Dafny *et al*. 2006) and Dalha Basalts in Djibouti, Africa (Jalludin 1994). These geological settings are likely to develop aquifers in their domains because fracturing in magmatic deposits develops naturally through time by cooling and tectonic processes. By the other hand, large aeolian deposits are older, but they can also be coeval with those large igneous provinces developing fractured, and granular aquifers directly juxtaposed one another (Almeida and Melo 1991; Scherer 2000,2002).

The area studied (Fig. 1) herein approaches the Serra Geral Plateau, part of the Paraná-Etendeka Province in southern Brazil, and includes two aquifer systems: Guarani and the Serra Geral. Geologically, they represent a continental succession formed by hundred meters thick sandstones of the Botucatu Formation, a large aeolian dune field deposits developed in center-south of South America during Jurassic-Cretaceous (Scherer 2000). It passes upward to a hundred-to-thousand meters succession of basalt-to-riodacite magma flows recorded as Serra Geral Formation (Schneider *et al*. 1974), developed as a response of the Gondwana breakup in Lower Cretaceous (Turner et al. 1994; Renne *et al*. 1996). The Botucatu Formation is the central unit of the granular Guarani aquifer system

(GAS) whereas Serra Geral Formation encompasses the fractured one (SGAS). The contact between both aquifers is not well known under the hydrogeological point of view, especially in terms of storage, flow, and the physical connexion between them (Uhl and Joshi 1986; Fernandes *et al*. 2012,2016, Gastmans *et al*. 2016).

The main difference between the two aquifers is the type of porosity. GAS has a classical primary intergranular porosity developed by depositional and diagenetic processes. SGAS has secondary fracture porosity generated during magma cooling, and tectonic processes and also porosity associated with amygdaloidal vesicles developed in the upper portion of magma flows by degasification (Domenico and Schwartz 1990; Jalludin and Razack 1994; Machado 2005). These types of porosity control the behavior of each aquifer but other factors also have to be considered, as the influence of tectonic on development of structures and connexion of fractures, geomorphologic patterns, and lithological characteristics in different scale, as a way to understand the different productivity of wells in places where there are the two aquifers. Thus, the main goal of this study is to test if the granular and fractured aquifers work effectively as different hydrogeological compartments and how tectonic, structural, lithological, and diagenetic characteristics act to modify the behavior and productivity of the groundwater in these aquifers.

(Insert Fig. 1)

2. The Geology of the Paraná-Etendeka Province and related Aquifer Systems

2.1. General aspects

The Paraná-Etendeka Province records volcanic processes occurred between in the Lower Cretaceous and released a volume of basic-to-acid magma up to $1x10^6$ km^3 (Erlank *et al*. 1984; Peate 1990; Turner *et al*. 1994; Renne *et al*. 1996; Jerram et al. 2005). Covering an area up to $1x10^6$ km^2 and with thickness ranging from 300 to more than 1500 m, these rocks represent the product of a Large Igneous Province (LIP) developed between 135 and 130 M.y. (Turner *et al*. 1994; Renne *et al*. 1996). This magma flooding spread over erg-type desertic environments fed by deep fractures into the crust as a result of the tectonic processes involved in the Gondwana breakup. The release and spreading of magma onto the surface had as the primary control the position of crustal weakness zones as well as the

regional dip, the relief associated with the dune fields and the position of the water bodies (Jerram *et al*. 2005). This association records a succession characterized by aeolian well sorted, fine-grained quartzous sandstones named as Botucatu Formation in Brazil (Schneider *et al*. 1974, Scherer 2000) and Etjo Formation, Huab Basin, in Namibia (Jerran *et al*. 1999) overlain by basic-to-acid lava flow deposits (locally with interbedded sandstones) of the Serra Geral Formation in Brazil (White 1908; Schneider *et al*. 1974) and Awahab Formation in Africa (Jerran *et al*. 1999). In the first events of the magmatism, basaltic lavas had direct contact with the underlying sands, and the lava-sediment interaction preserved many geomorphologic features of the paleo desert (Mountney *et al*. 1999; Jerram and Stollhofen 2002; Scherer 2002).

The extensive sandy deposits reported as Botucatu Formations is a widespread litostratigraphic unit in the Paraná Basin, distributed about 840 km^2 in Paraguay, Uruguay, and center and south of Brazil (Scherer 2000). It is the central unit of the GAS, constituted by metric to dozen of meters cross stratified Jurassic aeolian sandstones, characterized by well sorted, high sphericity, subrounded to well rounded, very fine-to-medium grains of quartzous to arkosic composition with siliceous, carbonatic and ferruginous cement and primary porosity of the type intergranular. The Botucatu Formation can reach more than 600 meters of maximum thickness (Milani *et al*. 2007) but it is quite variable due to erosion caused by tectonic uplifts and preserved morphology of the dunes with dozen of meters height reaching in general 200 to 300 m (Araújo *et al*. 1995, Machado 2005). These conditions establish the contact between the units Botucatu and Serra Geral in very different altimetric position even in the same study area. Under a productivity point of view, the GAS presents 48 km^3 of water storage, average porosity of 17 %, hydraulic conductivity ranging from 0.01 to 4.6 m/s, and specific capacity of 4 m^3/m/h, which include it as one of the larger hydrogeological systems of South America (Araújo *et al*. 1995,1999; Boscardin Borghetti *et al*. 2011; Machado and Freitas 2005; Heine 2008).

Volcanic rocks overlying the aeolian deposits throughout Paraná and Huab basins are nowadays as Serra Geral Formation (White 1908; Schneider *et al*. 1974). The composition ranges from ultrabasic (Lomba Grande Facies), basic (Gramado Facies) to acid (Caxias Facies), among others, from the base to the top, respectively. In the study area, basalts and riodacites predominate in the volcanic succession which also has some loose sandstone intercalations, a product of the aeolian-erg processes developed

after each lava flow, non-lithified because of rapid burial by other lava flows (Petry *et al*. 2015; Reis *et al*. 2014).

2.2. Compartmentalization and connexion of the Guarani and Serra Geral Aquifer Systems

Lava flow and cooling in the surface include volumetric contraction after decreasing of the temperature and development of vertical fractures that can connect one another generating the hexagonal pattern known as columnar disjunction. Desgasification is another feature resulting from magma decompression that promotes the accumulation of gas bubbles at the top of each lava flow deposit. It creates a complex porous system formed by vesicles and amygdales limited above by (quasi)horizontal surface that boundary the top of the lava flow. The arrange of fractures and vesicles represents the pore system of the magmatic domain. Vesicle-dominated zones have high permeability when they are connected, but they can be almost impermeable if they present infilling by secondary minerals (Naik *et al.* 2001). If there is water inside vesicles, joints can connect horizontal-and-vertically the water stored in different vesicular zones (Kulkarni *et al*. 1997; Johnson *et al*. 2002).

The succession formed by several lava flows develops sets of fractures as a response to the tectonic events that affect the deposits after cooling. The connexion of joints of different orientation tends to increase permeability as well as faults can connect different joint sets, increasing permeability a lot (Jalludin and Razack 1994; Rebouças and Fraga 1988). In specific cases, faults have a behavior of permeability barrier caused by fine-grained material, generated by weathering and infilling the open space along the fault plane and the damage zone.

The combination of fractures and vesicular zones constitutes the primary conduits for groundwater flow in basaltic aquifers like those of the Serra Geral Aquifer System (SGAS) (William *et al*. 2012). The fractures developed from the tectonic events resulted from the stress propagated along the entire succession but affecting rocks differently with different rheological characteristics. Thus, fault zones promote compartmentalization of the aquifers, and joint sets can propagate along juxtaposed aquifers connecting them (Fernandes *et al*. 2012,2016) and increasing the groundwater productivity (Uhl and Joshi 1986). In these cases, connected aquifers show composition resulting from the mixture of waters enriched by elements derived from the minerals and weathering products of each geological context (William *et al*. 2012; Gastmans *et al*. 2016).

142 The compartmentalization and connexion of the GAS and SGAS are controlled and influenced in
143 basin scale by Precambrian fault zones present in the Paraná Basin's basement reactivated along the
144 Phanerozoic (Fulfaro *et al*. 1982; Araújo *et al*., 1995). More specifically in southern Brazil, Machado
145 (2005) recognized four main blocks in the GAS limited by NE-SW and NW-SE lineaments. In a more
146 local scale of analysis, aquifer show specific characteristics that must be considered for
147 compartmentalization analysis, such as diagenetic aspects, that become sandstones hard enough to be
148 fractured. The controls of the compartmentalization are fundamental to understand very low productivity
149 or even flow rate of about 60 m^3/h and specific capacity of 3.35 m^3/h/m (Machado 2005). The complex
150 nature of the compartmentalization results of thickness variation by geomorphological paleosurfaces or
151 structural highs, fault zones, and erosion in the border of the basin (Soares 2008).
152 The relationship between GAS and SGAS has the thickness and type of fractures of the Serra Geral
153 Formation as the primary control of the confinament and recharge of the GAS (Wanfried 2010). From
154 studies in southeastern Brazil at Ribeirão Preto, Fernandes *et al*. (2012) infer that vesicular basalts in
155 the top of lava flow act as regional hydraulic barriers because the cooling processes do not permit the
156 fracture propagation beyond each lava flow, avoiding the fracture propagation until the underlying
157 sandstones of the GAS. However, the vertical connexion promoted by joints and faults supplies water
158 from the SGAS to the GAS in the sites where deformation and dips are higher than in surrounding areas.
159 Sites with deformation and dips higher are favorable to have a vesicular zone and interbedded sandstones
160 ("intertrappe sandstone" according Fernandes et al. 2016) connected to the horizontal joints where water
161 naturally accumulates (Fernandes *et al*. 2012,2016). The main patterns are those of NNE, NW, and ENE
162 in the region of Ribeirão Preto and NNE, WNW, and NE in the region of São Paulo (Fernandes *et al*.
163 2016).
164 More specifically in the study area at the Rio Grande do Sul, south Brazil, Reginato and Strider
165 (2006) indicated connexion the GAS and SGAS by the NE and NW lineaments, with the NW ones being
166 more productive than the NE. Reginato *et al*. (2013) point out that the aquifer connexion is also detected
167 by hydrochemical analysis due to the hydraulic charge differences and sodium bicarbonate, sodium
168 chloride, or sulfate-enriched composition where GAS is confined. Matos *et al*. (2018) identified
169 structural lineaments with NS, ES, NW, and, subordinately NE orientations, corroborating the lineament

patterns identified by Heine (2008) in the sediment-lava thermal metamorphism contact between GAS and SGAS.

The mixture of water of the GAS and SGAS showed by hydrochemical and isotopic composition also indicates the groundwater flow associated with the principal rivers of the area along valleys that cut the basalts and sandstones influenced by the relief (Gastmans and Chang 2012; Gastmans *et al*. 2016). These flow paths modify the groundwater composition between the recharge and discharge areas. Feldspar grains dissolution in the recharge area release ions K+, H4SiO4 in solution after hydrolysis and kaolinite precipitated in the pore system generating secondary porosity as microporosity and moldic pore where the aquifer is confined (França *et al*. 2003, Gastmans *et al*. 2010). The more is the thickness of the volcanic rocks the less is the weathering affecting the GAS' sandstones, decreasing feldspar dissolution, sílica release, and the amount of cement, i.e., promoting the best groundwater circulation. This fact also explains the natural tendency of quartzous sandstones in outcrops and arkoses in the subsurface (França *et al*. 2003).

3. Material and Methods

This study had three main analysis developed and integrated involving petrology, structural geology, and hydrogeology. SRTM (Shuttle Radar Topography Mission) provided the regional structural trends from images with 30 m of spatial resolution. Using shaded relief maps in scales 1:750,000, 1:400,000, 1:250,000, and 1:100,000, structural lineaments were demarcated in the ArcMap® 10.3 version in order to calculate orientation and length. The analysis and integration of geological data and elevation of the contact Botucatu-Serra Geral allowed demarcation of six structural blocks.

The measurement of joints using compass revealed the local structural patterns of both Botucatu Formation and Serra Geral Formation. Structural measurements collected inside the well from 360° images acquired by an Optical Televiewer (OTV) allowed to analyze the fracturing pattern in both units and to measure planar structures like joints and bedding surfaces using the WellCAD® software. Rosette diagrams and stereograms plotted in Stereonet® represented the results in Schmidt's lower hemisphere projection.

The petrological aspects of the volcanic and sedimentary rocks analyzed from the mapping along natural outcrops, quarries, and roadcuts included descriptions and measurements in the outcrop, from hand samples, and of thin sections. The fieldwork has permitted mapping the Botucatu and Serra Geral units and to mark the altimetric position of its contact, to demarcate the base and top of lava flows and their vesicular zones, to acquire structural data, and to collect samples for detailed petrographic analysis. Sixteen thin sections of sandstones from the six different structural blocks were made with impregnation of blue epoxy resin to enhance porosity.

Textural and compositional aspects involving grains, matrix, cement, and porosity were analyzed in optical microscope Zeiss Axio Lab with a scientific camera mounted into an acquisition system of 12MPx operated by the Zen software. Descriptions included grain size variation, sorting, roundness, sphericity, types of porosity and grain and cement composition. The classification of sandstones followed the proposition of Folk (1954). The quantification by modal counting of 300 points per thin section allowed the comparison and identification of different characteristics of each block inside the study area. The relationship between detrital composition, type of cement, and porosity were demonstrated by the quantification in microscopical analysis and helped to evaluate the permeability barriers of microscale.

The hydrogeological characterization used a well data inventory from the Brazilian Groundwater Information System (SIAGAS) of the Brazilian Geological Survey (CPRM), from the Companhia Riograndense de Saneamento (CORSAN), from the Secretaria de Habitação e Saneamento (SEHABS), and database from private institutions. Six hundred wells were analyzed, and 375 of them selected for data compilation. Three groups of wells had been selected based on the water inflow as follow: 99 wells with water inflow from the SGAS, 175 from the GAS, and 101 from both SGAS and GAS. The primary data were the elevation of the water table and the hydrodynamic parameters of flow rate and specific capacity used in maps performed in the ArcMap 10.3 software interpolated with IDW (inverse of distance weighted). The hydrochemical data after processing in Qualigraf 2017 was plotted in the Piper diagrams to classify the groundwater. The altimetric cote of the Botucatu-Serra Geral and the position of water inflow in both aquifers were processed using mean and median and represented in two geological sections drawn in *Adobe Illustrator® 2018.*

The integration of all data collected was fundamental to propose geological sections and a conceptual framework of the hydrogeological compartmentalization, aquifer connexion, and groundwater flow in the study area. Additional data must be continuosuly inserted in the database to improve and to test the accuracy of the model.

4. Results

4.1 Regional Structural Trends

Lineaments identified in scale 1:750,000 present orientation trends NS, WNW (N80-90W), ENE (N80-90E), NW (N30-45W), NE (N40-55E), whereas lineaments in scale 1:250,000 present orientation trends NNW (NS-N10W), NNE (NS-N20E), ENE (N80E-EW) and ENW (N80W-EW) (Fig. 2). The trends of lineaments in both scales indicated a set of six lineaments with more than 20 km length present in valleys of the most important rivers as the Sinos River, that crosses three major lineaments with EW, N70W, and N70E orientations (Fig. 2).

(Insert Fig. 2)

4.2 Aquifer System Characterization

Ninety-nine wells have water inflow in the Serra Geral Aquifer System (SGAS) permitted identify groundwater flow to southeast and subordinately to east (Fig. 3). The recharge zone is in the north of the study area while the discharge zone is along the Sinos River together with the main tectonic lineament. Seven wells have flow rates higher than 30 m^3/h in the northwest and southeast areas, including the higher flow rate of the study area, 66 m^3/h in Morro Reuter municipality. The lowest flow rates are in the center-south region, and specific capacity ranges from 0.1 and 1 $m^3/m/h$, but values higher to 2 $m^3/m/h$ were recorded in 14 wells in the northwest and southeast of the area. More detailed productivity data about the SGAS are available in Table 1. Hydrochemical analysis plotted in the Piper chart indicated 44% of sodium bicarbonate water, sodium sulfate (11%) and the others as bicarbonate of mixed composition.

The data processing in 175 wells with water inflow in the Guarani Aquifer System (GAS) revealed the main groundwater flow to the southeast, associated with the Sinos River, but there is also flow to

252 the north towards the Rio Paranhana, associated with structural lineaments presented in the Fig. 3. The
253 recharge zones are located in the northwest and center-south, whereas discharge zone is in the southeast.
254 Ten wells have flow rates higher than 30 m^3/h in the northwest, southeast, and center-south areas
255 including the higher flow rate of the area, 44 m^3/h in the Igrejinha municipality. The lowest flow rates
256 are in the center-south of the area, and specific capacities range from 0.1 to 1 m^3/m/h, but values of
257 about 2 m^3/m/h were recorded in 8 wells in the center-south, northeast, and northwest of the area. The
258 maximum value of the flow rate is 5.3 m^3/m/h in the northwest. More detailed productivity data about
259 the GAS are available in Table 1. Hydrochemical analysis plotted in the Piper chart indicated 20% of
260 calcium bicarbonate water, 22% of sodium bicarbonate and the others as bicarbonate of mixed
261 composition.

262 The data analysis of 101 wells with water inflow in the fractured SGAS and granular GAS showed
263 the main groundwater flow to Sinos River. 93% of the wells have water inflow in the surface that
264 represents the contact of the Botucatu Formation and Serra Geral Formation. Ten wells have a flow rate
265 higher than 30 m^3/h located in the northwest and center-north of the area. Flow rates higher than 50 m^3/h
266 are in the southeast with the highest value of 61 m^3/h. The lowest flow rates are in the center-south of
267 the area and are lower than 10 m^3/h.

268 Specific capacities range from 0.1 to 1 m^3/m/h, but values of about 2 m^3/m/h were recorded in 13
269 wells in the northwest and southeast. More detailed productivity data about the GAS/SGAS are available
270 in Table 1 and Fig. 3. Hydrochemical analysis plotted in the Piper chart indicated 31% of calcium
271 bicarbonate water, 10% of sodium bicarbonate and the others as bicarbonate of mixed composition.

272 (Insert Fig. 3 e Table 1)

273 *4.3 Hydrogeological Compartmentalization*

274 4.3.1 Sandstone-Basalt Lithological Contact

275 The identification of structural lineaments in different scales together with geomorphological
276 patterns and the position of the main rivers in the study area suggested the existence of hydrogeological
277 compartments. The comparison of an undoubtful surface along the whole area in terms of altimetric
278 position could validate this possibility. Thus, the contact between Botucatu and Serral Geral formations
279 allowed this comparison and revealed the presence of six structural blocks identified as A, B, C, D, E,

and F as shown in the Fig. 4. The contact Botucatu-Serra Geral range almost 400 m in elevation, from the minimum -156 m in the southeast to the maximum 238 m in the northwest of the area according to the data available in Table 2. This variation of the elevation position of the contact is directly related to each structural block above mentioned because of the relative vertical movements among them.

(Insert Fig. 4 e Table 2)

4.3.2 Hydrodynamic Characterization

The hydrodynamic data about flow rate and specific capacity of all productive wells from both GAS and SGAS aquifers (Table 3) reveals that block F is the most productive because it is coincident with the discharge zone of both GAS and SGAS, with a maximum flow rate of 61 m^3/h and a maximum specific capacity of 7.2 $m^3/m/h$. The block A is the second most productive with maximum flow rate of 46 m^3/h and specific conductivity of 10 $m^3/m/h$.

With mean and median values of flow rate and specific capacity close to the block A, block E, in the northwest of the area does not record high values for flow rate (>15 m^3/h) and high specific capacity (>1 $m^3/m/h$) which determine intermediary productivity. Block C, in the center-north of the area, is also of intermediary productivity because there is no SGAS in the area and high flow rate and specific conductivity occur only in the GAS. The block D in the center-south presents the lowest productivity, with a flow rate of less than 10 m^3/h and a maximum specific capacity of 0.25 $m^3/m/h$. In the northwest, the block B has high productivity, but few wells are crossing the contact Botucatu-Serra Geral because the area is the highest in elevation, where predominates the volcanic rocks and SGAS is the unique or the more productive aquifer in that block.

(Insert Table 3)

4.3.3 Structural Trends in Sandstones and Basalts from Surface and Subsurface Data

The field measurement of planar surfaces taken from the Botucatu Formation sandstones and the Serra Geral volcanic rocks in the six structural blocks allowed to define the structural pattern of the joints to each one as shown in the Fig. 5. The comparison of data graphically represented by rosettes diagrams for all blocks indicated main orientations ENE (N70E-EW), NNW (NS-N20W) and WNW

306 (N70W-EW) for the basalts. For the sandstones, the main orientations are WNW (N70W-EW), ENE
307 (N70E-EW), NE (N40-60E) and NW (N40-50W).
308 (Insert Fig. 5)
309 The analysis of each structural block allowed identifying the relationship between the joint
310 orientation pattern in the sandstones and basalts to verify the potential connexion between aquifers. In
311 many blocks, the joint pattern is similar in one joint set at least. The block A exhibit preferential trend
312 to ENE, WNW, and NE for both aquifers but GAS has more expressive joint set to NE (N30-50E) (see
313 Fig. 5). The main lineaments of this block have the some diferents orientations patterns NW (N30-40W),
314 NNW (N10-20W), and ENE (N70E-EW). The block B presents more data dispersion in the joint sets,
315 but the typical pattern for both aquifers is NW. The NNW trend is expressive for the SGAS but not for
316 GAS. The major lineaments of this block have orientation ENE (N80E-EW), WNW (N70W-EW) and
317 NNE (NS-10W) (see Fig. 5).
318 Blocks C and D do not show a direct relationship between the joint sets of GAS and SGAS. The
319 joints of the sandstones in C have a well-defined orientation to WNW. In block D, there are little
320 structural data for GAS because sandstones are few fractured. SGAS also had a limited structural
321 sampling because basalts are quite rare in this block. The main orientation patterns for GAS and SGAS
322 in block D are NE (N30-50E), and WNW (N70W-EW) and NE (N50-70E), respectively. Lineaments in
323 the block C are oriented NW (N40-50E) and NNE (N10-20E) and in the block D are NW (N30-40W),
324 WNW (N80W-EW), and NNW (NS-N20W). Block E has the ENE structures present in both aquifers,
325 with GAS presenting a N70E-EW and N40-60W primary orientations while SGAS presents NE and
326 NW pattern of approximately N50-70E and N10-20W. The main lineaments are ENE (N70E-EW),
327 WNW (N80W-EW) and NNW (N10-30W). Block F has a strong relationship between ENE (N60-80E)
328 and N30W joints for GAS and SGAS, but sandstone has a WNW joint set not observed in the basalts.
329 The main lineaments in F are WNW (N60-70W) and NW (N10-30W).
330 A subsurface sampling of structural data was obtained from optical logging of the Cantagalo well
331 located at UTM coordinates (22J, 544136E, 6716724N, 232 m), Block E, Rolante Municipality (Fig. 6).
332 The measurement of joints along the whole well reveals two orientation trends in both aquifers for EW
333 and, subordinately, NE. Sandstones of the GAS have orientation trends to NE (N40-50E), and WNW

(N80W-EW) and basalts of the SGAS present joints NW (N20-30W), NE (N50-60E), and WNW (N80W-EW). Figure 6 shows three zones of interest identified along the well. Rosette diagrams display the trend WNW (N70W-EW) as the primary joint set associated with minor local variations NE (N60-80E). In the zone of the contact Botucatu-Serra Geral, there are joints with a prominent trend NNE (NS-N10E).

(Insert Fig. 6)

4.3.4 Description of the Structural Blocks

The mapping of the study area (Fig. 1) provided geological characteristics of each structural block in terms of rock composition and structural pattern of the lava flow zones. Moreover, we identified different fracturing degree in both sandstones and basalts in all the six structural blocks (Table 5).

(Insert Table 5)

The block A shows basalts with prominent fractures associated with columnar disjunction and joints oriented to WNW and NE (Fig. 7A) and sandstones with large, metric-to-decametric cross stratifications, with water inflow associated with cross sets or diagenetic features as tafoni (Fig. 7B). There are few outcrops of sandstones in block B. One of them is shown in Fig. 7C, where it is evident the contact of intercalation of sandstone between lava flows ("intertrappe sandstone"). Sandstone in these cases usually is water saturated and associated with reddish vesicular zone derived from weathering of basalts displaying joints with NW and NE orientation (Fig. 7D). Locally, there is thermal metamorphism features in the contact sandstone-basalt. Upward, in the domain of the volcanic rocks of Serra Geral Formation it is possible to observe the contact between lava flow zones where the trend northeast is similar in the zones 1 (vesicular-amygdaloidal) and 3 (vertical joints), and the trend east-west is similar in the zones 2 (horizontal joints) and 3 (Fig. 7E). Some minerals present as amygdales indicate connexion of the vesicular zone by the joints and fluid percolation inside vesicles. Some sandstone exhibit intense fracturing as in Fig. 7F. In the north of this block, in higher altitudes, crops out more acid volcanic rocks as tabular riodacites of the light color of the Caxias Facies (Fig. 7G).

(Insert Fig. 7)

Block C, in the center-north of the area, shows basalts with active weathering features associated with the vesicular zones (Fig. 8A). Horizontal joints (1) and verticalized ones (2) with trends NW and

NNW are very prominent in basaltic rocks of this region. Cross-stratified sandstones have the same orientation pattern to NE and WNW of the basalts, but its expression is different in each rock (Fig. 8B-C). The influence of joints in sandstones of the Botucatu Formation is evident through observation of cement distribution along stratifications. Iron oxides and hydroxides of yellowish color occur in levels of high permeability associated with coarser-grained sands (grain flow) in the region of Três Coroas, where there are not large joints crossing the outcrop. In the nearby area of Igrejinha, the same type of sandstones present close-spaced fractures and there is not evidence of cemented level as observed in the area of Três Coroas (Fig. 8C). A high degree of fracturing expressed as columnar disjunction and one expressive NNW fault crossing the entire lava flow succession in shown in the Fig. 8D.

In the area center-south, block D, outcrops of basalts are quite rare although the area is more elevated in altimetry. Only one basalt outcrop with well developed vesicular zone was visited in this area and, therefore, the number of structural data is limited. Sandstones exhibit few joints and high content of whitish kaolinite and orange-to-black iron oxides and hydroxides as type of cement - the Fig. 8E-F-G present examples of quarries of sandstones where expressive clay occurrences constitute permeability barriers. Joints filled with ?smectite clay mixtures oriented to NW (N30W) and NE (N65E) promotes lateral segmentation of the permoporous system (Fig. 8E). Kaolinite occurs inside the pores as patches well developed, but it is also distributed along the stratification planes (Fig. 8F-G).

(Insert Fig. 8)

The block E has limits in the northeast of the study area, and the joint sets are NNE, NE, and NW. During the fieldwork, it was possible to observe water percolation along a joint NE (N30E) and NW (N60W) (Fig. 9A). It was also possible to evaluate that two sandstones interbedded within basalts and the contact between Botucatu and Serra Geral formations sandstone are prone to have water inflow as demonstrated by humid and water saturated zones (Fig. 9B) where locally joints have orientation ENE and NW. In the block F, joint sets in sandstones occur near the contact between sandstones and lava flow basalts with columnar disjunction (Fig. 9C) while sandstones occur near basalts with well-developed joints (Fig. 9D). Sandstones and basalts have joint trends to WNW, NW and ENE, respectively. The contact between sandstones and a very altered vesicular basalt crops out along the roadcut BR-290 (Fig. 9E) and exhibit joints oriented between ENE and WNW. In this region was

possible to observe water percolation and humid zones in the rocks, with joints oriented WNW, ENE and NNW.

(Insert Fig. 9)

4.3.5 Petrography of sandstones

The microscopic characterization of sandstones provided textural and compositional characteristics useful to understand the relationship between porosity and cementation in samples collected in different structural blocks, as shown in Fig. 10 and Table 4.

(Insert Fig. 10 and Table 4)

In the block A, sandstones are quartzous, and samples were collected in order to represent different situations as the thermal metamorphism close to the contact sandstone-basalt and friable samples with apparent high porosity where large pores in joints create conduits for active water circulation (Fig. 10A). The samples of the block B are sandstones interbedded in basalts (see Fig. 7D), characterized as an arkose and porosity connexion limited by cement among the grains (Fig. 10B). The block C presents arkoses that show granulometric intercalations interpreted as a product of grain flow and grain fall processes. Porosity ranges between 2% (Fig. 10C) and 13.3% (Fig. 10D) as a function of the degree of joints, and iron oxides cement distributed in the pore system.

Three samples of sandstones analyzed by thin sections showed quartzous composition in the block D. The worst porosity is 3% in sandstones with evident granulometric intercalations associated with grain fall and grain flow processes but with conspicuous cementation by iron oxides and hydroxides (Fig. 10E). The most porous samples have 11.8% of intergranular porosity, but it also presents kaolinite distributed in whitish levels, as shown in the figures 8E-G, that become water percolation confined and restricted. Kaolinite as cement can reduce porosity to low values as 1.3% by filling of almost all the intergranular pores (Fig. 10F).

Thin sections of the block E analyzed samples collected in the outcrop shown in figure 9B. The composition is subarkosean, and porosity of 12.5% derives from proper sorting, well-rounded grains, and interstitial space not filled by cement (Fig. 10G). Three thin sections from the block F collected below, near, and above the sandstone-basalt contact with composition between arkose and subarkose and a variable degree of fracturing shows very low porosity of 1.3% in sandstones (Fig. 10H). Very

418 close to the contact sandstone-basalt the porosity is 17% and is well connected by microfractures (Fig.
419 10I) while sandstones intercalated within the basalt lava flows and well evident joint sets (see Fig. 9C)
420 has 14% of porosity (Fig. 10J).
421
422 **5. Discussion**
423 Within a regional context, the main lineaments represent fault systems with preferential orientations
424 to NNW NNE, ENE and ENW derived from reactivation of ancient Precambrian structures and from
425 stress-strain associated with the Gondwana breakup between Jurassic and Cretaceous (Milani and
426 Ramos 1998; Milani *et al.* 2007). These main orientations promoted relative movement of the structural
427 blocks in the study area and generation of joint sets as a product of stress propagated in the rocks through
428 time. The relative movement among blocks is the primary control in the compartmentalization of both
429 GAS and SGAS in the study area and corroborates previous interpretations of Araújo *et al*. (1995),
430 Machado (2005), and Soares (2008) in other areas of the Paraná Basin. In the study area, the fault
431 systems are associated with the geomorphologic expression of features as the valleys of Sinos, Rolante,
432 Rio Paranhana and others rivers.
433 The altimetric position of the contact Botucatu-Serra Geral ranges about 400 meters and is a function
434 of the synsedimentary or a posteriori relative vertical movement of each structural block (Araújo *et al.*
435 1995; Scherer 2002) and also of the altimetric variation of giant decametric dunes of the Botucatu
436 palaeo-desert. The analysis of the aquifer in the geological sections A-A'(NW-SE) and B-B'(WNW-
437 ESE) (Fig. 11) shows their relationships with the structural blocks A to F and the variation of the
438 elevation of the Botucatu-Serral contact. The surface that defines this lithological contact dips differently
439 in each block, as follows: to SW in the block A, W in the block B, probably to S in the block C, SW in
440 the block D, NW in the block E, and SE in the block F. These dips associated with the potentiometric
441 surfaces helped to identify the recharge zones in the northwest and center-south. Discharge zones occur
442 in the southeast, where the groundwater flow is parallel with the EW orientation of the Sinos River.
443 (Insert Fig. 11)
444 The integration of surface and subsurface optical logging structural data corroborates the pattern of
445 the predominance of EW and NE joints for sandstones and basalts of the block E. It attests the validity

446 of surface structural data for geological and hydrogeological purposes, *i.e.,* tensional surface noise does
447 not alter structural data pattern significantly. The comparison of joint measurements and regional
448 lineaments patterns corroborates connexion of structures in different scales both in the GAS and SGAS
449 as evidenced by different geomorphological patterns observed in the Sinos and Rolante rivers.
450 Furthermore, it agrees with structural analysis previously published by Reginato and Strider (2006),
451 Heine (2008), and Matos *et al*. (2018) in the Rio Grande do Sul state, and Fernandes *et al.* (2012,2016)
452 in São Paulo state.

453 Flow rate and specific capacity of wells producing in the GAS and SGAS indicate more groundwater
454 production in wells that drilled both aquifers. The more productive regions are in the blocks A and F, in
455 the northwest and southeast, respectively. They present high porosity associated with joints and low
456 degree of cementation, *i.e.*, they have the behavior of dual porosity, primary and secondary (Machado
457 2005). The intercalations observed in wells of the geological section B-B' suggest that the same joint
458 sets propagate both in the sandstones and in the basalts promoting a strong connexion of the aquifers
459 (Fig. 11). In the block F, the high productivity is a product of the discharge zone and high degree of
460 fracturing that increase porosity in arkose sandstones from 1.3% in purely granular to 17% in open joints
461 just below the contact sandstone-basalt. A sample of the block C with 13.3% of porosity in arkhosean
462 sandstone with a dense network of joints corroborates that connexion promoted by this type of structures
463 allows more effective water percolation into the rock, avoiding cement precipitation and keeping
464 intergranular and fractures opened. In areas with a low degree of joints, as in the block D, sandstones
465 have groundwater that migrates slowly inside the pore system due to the restriction of circulation
466 imposed by the types of cements and pore throats.

467 The integration of all results obtained from a multiscalar approach supported the development of a
468 conceptual hydrogeological model to the study área (Fig. 12). The compartmentalization of the aquifers
469 and the subdivision in structural blocks show the geomorphological expression and the range of
470 elevation of the GAS/SGAS contact. Additionally, it demonstrates the orientation of the main tectonic
471 structures that control this contact.

472 Insert (Fig. 12)

6. Conclusions

Geological analysis of tectonic, structural, sedimentological, petrographic, and diagenetic aspects helped to understand hydrogeological data of productivity and integrate one another. All the six structural blocks have their limits defined by fault zones expressed as regional lineaments whose fracturing pattern allowed the connexion of Guarani and Serra Geral Aquifer Systems. Compartmentalization defines the complex behavior of aquifers in terms of productivity. 93% of the wells drilled in both granular and fractured aquifers showed water inflow the contact sandstone-basalt attesting that this surface develops high storage and flow and therefore constitutes a very reliable indicator of good productivity. This is particularly important because this contact ranges more than 400 meters in elevation as a consequence of vertical displacement along with fault systems and paleo-geomophological surfaces and any predictive criterium must consider this condition.

The more productive blocks have a relationship with many different controls as the presence of the contact between aquifers, the recharge x discharge zones, geomorphology, and the connexion of the aquifers by the same fracture sets. The internal network of joints in basalts created by columnar disjunction, tectonic joints, contact of different lava flows, water stored in vesicular zones, and intergranular porosity dependent of both degree of cementation and water percolation in joints also influence the productivity of groundwater. The integration of all results and discussion presented in this study supported the proposition of a hydrogeological conceptual model based on many different interdependent factors. The factors controlling the productivity in each structural block have to be detailed with an integrated approach to understand the complexity of the aquifers better and provide reliable predictions.

7. Acknowledgments

RCS thanks the financial support received as a scholarship from PROSUC/CAPES Program. PPGEO-UNISINOS and IPH-UFRGS provided laboratory and fieldwork facilities as software, sample preparation, and vehicles. The technical staff of LASERCA (Gustavo, Graciela, Diego, Milena, Gabriel, and Leonardo) and Thin Section and Sample Preparation Laboratory (Lauro Rosa and Adriano Xavier) were fundamental to achieve excellent results in this research. We thank especially George

Olufunmilayo Gasper for helping with the OTV logging acquisition and WellCad data interpretation. Mauricio Righi helped with petrographic analysis and modal counting. The research group VizGEO, especially Lais V. Souza, provided facilities and scientific discussions. We thank the Brazilian Geological Survey (CPRM-SIAGAS) as well as CORSAN, SEHASB, and HidroGeo Perfurações Ltda for providing well data. José Luiz Flores Machado and Raquel Binotto critically read and improved a previous version of the manuscript. FMWT thanks the grant of the Brazilian Council for Scientific and Technological Development (CNPq proc. 311204/2017-1).

8. References

Almeida FFM, Melo MS (1981) A Bacia do Paraná e o vulcanismo mesozoico. Mapa Geológico, Instituto de Pesquisas Tecnológicas do Estado de São Paulo, Brazil. 1: 46-81

Araújo LM, França AB, Potter PE (1995) Aquífero Gigante do Mercosul no Brazil, Argentina, Uruguay and Paraguay: Hydrologic maps of the Formations Botucatu, Pirambóia, Rosário do Sul, Buena Vista, Misiones and Tacuarembo. Universidade Federal de Paraná, Biblioteca de Ciência e Tecnologia, Centro Politécnico, Curitiba, p 1-16

Araújo LM, França AB, Potter PE (1999) Hydrogeology of the Mercosul aquifer system in the Paraná and Chaco-Paraná basins, South America, and comparison with the Navajo-Nugget aquifer system, USA. Hydrogeol J 7:317-336, doi: 10.1007/s100400050205

Boscardin Borghetti, JR Borghetti, NR, Rosa Filho, EF (2011) Aquífero Guarani: a verdadeira integração dos países do Mercosul. Edição da Autora

Dafny E, Burg A, Gvirtzman H (2006) Deduction of groundwater flow regime in a basaltic aquifer using geochemical and isotopic data: the golan heights, Israel case study. J. Hydrol. 330:506-524. doi: 10.1016/j.jhydrol.2006.04.002

Domenico PA, Schwartz FW (1990) Physical and chemical hydrogeology. John Wiley & Sons, 824 pp. doi: 0.1017/S0016756800019890

Erlank AJ, Marsh JS, Duncan AR, Miller RMcG., Hawkesworth, CJ, Betton, PJ, Rex DC (1984) Geochemistry and petrogenesis of the Etendeka volcanic rocks from SWA/Namibia Geological Society of South Africa Special Publication. 13: 195-245

Fernandes Negri FA, Azevedo Sobrinho JM, Varnier C (2012) Análise de fraturas dos basaltos do Aquífero Serra Geral e o potencial de recarga regional do Sistema Aquífero Guarani. Boletín Geológico y Minero. 123(3): 325-339

Fernandes AJ; Maldaner CH, Negri F, Rouleau A; Wahnfried I (2016) Aspects of a conceptual groundwater flow model of the Serra Geral basalt aquifer (São Paulo, Brazil) from physical and structural geology data. Hydrogeol J 24:1199– 1212. doi: 10.1007/s10040-016-1370-6

Folk RL (1974) Petrology of Sedimentary Rocks. Hemphill Publishing Co o, 1980. Print.

França AB, Araújo LM, Maynard JB, Potter PE (2003) Secondary porosity formed by deep meteoric leaching: Botucatu eolianite, southern South America. AAPG Bulletin 87(7):1073-1082. doi: 10.1306/02260301071

Fulfaro VJ, Saad AR, Santos MV, Vianna RB (1982) Compartimentação e evolução tectônica da Bacia do Paraná. Revista Brasileira de Geociências 12(4): 590-611

Gastmans D, Chang HK, Hutcheon I (2010) Groundwater Geochemical Evolution in the Northern Portion of the Guarani Aquifer System (Brazil) and its relationship to diagenetic features Applied Geochemistry. 25(1): 16-33. doi: 10.1016/j.apgeochem.2009.09.024

Gastmans D, Hutcheon I, Menegário AA, Chang HK (2016) Geochemical evolution of groundwater in a basaltic aquifer based on chemical and stable isotopic data: Case study from the Northeastern portion of Serra Geral Aquifer, São Paulo state (Brazil).J Hydrol. 535:598-611. doi: 10.1016/j.jhydrol.2016.02.016

Heine CA (2008) Análise de sustentabilidade de uso do sistema aquífero Guarani em Ivoti/RS. Unpublished PhD Thesis, Universidade do Vale do Rio dos Sinos, Brazil, 375 pp

Jalludin M, Razack M (1994) Analysis of pumping tests, with regard to tectonics, hydrothermal effects and weathering, for fractured Dalha and stratiform basalts, Republic of Djibouti. J Hydrol 155(1–2): 237–250. doi: 10.1016/0022-1694(94)90167-8

Jerram DA, Widdowson M (2005) The anatomy of continental flood basalt provinces: geological constraints on the processes and products of flood volcanism. Lithos 79(3):385–405. doi:10.1016/j.lithos. 2004.09.009

Jerram DA, Mountney N, Howell JA, Long D, Stollhofen H (2000) Death of a sand sea: an active aeolian erg systematically buried by the Etendeka flood basalts of NW Namibia. Journal of the Geological Society, 157: 513-516

Jerram. DA, Mountney N, Holzfoster F, Stollhofen, H (1999) Internal stratigraphic relationships in the Etendeka Group in the Huab Basin, NW Namibia: understanding the onset of food volcanism. Journal of Geodynamics 28 (4-5): 393-418. doi:10.1016/S0264-3707(99)00018-6

Johnson, GS, Frederick DB, Cosgrove DM (2002) Evaluation of a pumping test of the Snake River Plain aquifer using axial-flow numerical modeling. Hydrogeol J 10(3):428–437. doi: 10.1007/ s10040-002-0201-0

Kulkarni HSB, Deolankar A, Lawwani B, Joseph S (2000) Hydrogeological framework of the Deccan basalt groundwater systems, West-central India. Hydrogeol J 8:368-378

Kulkarni H, Lalwani A, Deolankar SB (1997) Selection of appropriate pumping systems for bore wells in the Deccan basalt of India. Hydrogeol J 5(3):75-81. doi: 10.1007/s100400050258

Katpatal AMP, Yashwant B, Bhushan RL (2014) A groundwater flow model for overexploited basaltic aquifer and Bazada formation in India. Environ Earth Science (72):4413–4425. doi: 10.1007/s12665-014-3342-2

Lindholm GF, Vaccaro JJ (1988) Region 2, Columbia Lava Plateau. The Geology of North America, Hydrogeology 10(2):37-50

Machado JLF (2005) Compartimentação espacial e arcabouço hidroestratigráfico do Sistema Aqüífero Guarani no Rio Grande do Sul. Unpublished PhD Thesis, Universidade do Vale do Rio dos Sinos, Brazil, 237 pp

Machado JLF, Freitas MD (2005) Projeto Mapa Hidrogeológico do Rio Grande do Sul: Relatório Final. Companhia de Pesquisa de Recursos Minerais (CPRM).

Matos AB, Reginato, PAR, Athayde GB (2018) Hydrogeological compartmentation of the Guarani Aquifer System in the serra geral escarpment in the northeast of RS. Águas Subterrâneas 32(1):130-139. doi: 10.14295/ras.v32i1.28965

Milani EJ (1997) Evolução tectono-estratigráfica da Bacia do Paraná e seu relacionamento com a geodinâmica fanerozóica do Gonduana Sul-Ocidental. Unpublished PhD Thesis, Universidade Federal do Rio Grande do Sul, Brazil, 255 pp

Milani EJ, Ramos VA (1998) Orogenias paleozóicas no domínio sul-ocidental do Gondwana e os ciclos de subsidência da Bacia do Paraná. Revista Brasileira de Geociências 28(4): 527-544.

Milani EJ, Melo JHG, Souza PA; Fernandes LA, França AB (2007) Bacia do Paraná. Cartas Estratigráficas. Boletim de Geociências da Petrobras 15 (2): 265-287.

Mountney N, Howell J, Flint S, Jerram DA (1999). Relating eolian bounding-surface geometries to the bed forms that generated them: Etjo Formation, Cretaceous, Namibia. Geology, 27 (2), 159-162. doi: doi.org/10.1130/0091-7613(1999)027<0159:REBSGT>2.3.CO;2

Naik PK, Awasthi AK, Anand AVSS, Mohan PC (2001) Hydrogeologic framework of the Deccan terrain of the Koyna River basin, India. Hydrogeol J 9:243-264. doi: 10.1007/s100400100123

Peate DW, Hawkesworth CJ, Mantovani MS, Shukowsky W (1990) Mantle plumes and flood basalt stratigraphy in the Paraná Basin, South America. Geology, 18(12):1223-1226. doi: 10.1130/0091-7613(1990)018<1223:MPAFBS>2.3.CO;2

Petry, K, Almeida, DPM, Zerfass H (2005) O vulcanismo Serra Geral em Torres, Rio Grande do Sul, Brasil: empilhamento estratigráfico local e feições de interação vulcano-sedimentar. Journal of Geoscience, 1(1):36-47

Rebouças AC, Fraga CG (1988) Hidrogeologia das rochas vulcânicas do Brasil. Águas Subterrâneas, (12):30-55.

Reginato PAR; Strieder AJ (2006) Caracterização estrutural dos aquíferos fraturados da Formação Serra Geral na região nordeste do estado do Rio Grande do Sul. Revista Brasileira de Geociências 36 (1): 13-22

Reginato PAR, Ahlert S, Schneider VE (2013). Caracterização hidroquímica do sistema aquífero Serra Geral na região nordeste do Rio Grande do Sul. Águas Subterrâneas 27(1):65-78. doi:10.14295/ras.v27i1.27061

Reis GS, Mizusaki AM, Roisenberg A, Rubert RR (2014) Formação Serra Geral (Cretáceo da Bacia do Paraná): um análogo para os reservatórios ígneo-básicos da margem continental brasileira. Pesquisas em Geociências 41(2):155-168. doi:10.22456/1807-9806.78093

Renne PR, Deckart K, Ernesto M, Féraud G, Piccirillo EM (1996) Age of the Ponta Grossa dike swarm (Brazil), and implications to Paraná flood volcanism. Earth and Planetary Science Letters, 144 (1-2): 199-211

Schneider RL, Mühlmann H, Tommasi RA, Medeiros RA, Daemon RF, Nogueira AA (1974) Revisão estratigráfica da Bacia do Paraná. Congresso Brasileiro De Geologia, 28(1):41-65

Scherer CMS (2000) Eolian dunes of the Botucatu Formation (Cretaceous) in southernmost Brazil: morphology and origin. Sedimentary Geology 137:63-84. doi: 10.1016/S0037-0738(00)00135-4

Scherer CMS (2002) Preservation of aeolian genetic units by lava flows in the Lower Cretaceous of the Paraná Basin, southern Brazil. Sedimentology 49:97–116. doi:10.1046/j.1365-3091.2002.00434.x

Soares AP (2008) Variabilidade espacial no Sistema Aquífero Guarani: controles estratigráficos e estruturais. Unpublished PhD Thesis, Universidade Federal do Rio Grande do Sul, Brazil, 196 pp

Turner SP, Regelous M, Kelley S, Hawkesworth C, Mantovani MSM (1994) Magmatism and continental brea-up in the South Atlantic: high precision 40 Ar -39Ar geochronology. Earth and Planetary Science Letters, 121:333- 348.

Uhl VWJR, Joshi VG (1986) Results of pumping tests in the Deccan Trap Basalts of Central India. J. Hydrol J 86: 147-168. doi: 10.1016/0022-1694(86)90011-9

Wahnfried ID (2010) Modelo conceitual de fluxo do Aquitarde Serra Geral e do Sistema Aquífero Guarani na região de Ribeirao Preto, SP. Unpublished PhD Thesis, Universidade de São Paulo, Brazil, 135 pp

Waichel BL, Lima EF, Viana AR, Scherer CM, Bueno GV, Dutra G (2012) Stratigraphy and volcanic facies architecture of the Torres Syncline, Southern Brazil, and its role in understanding the Paraná–Etendeka Continental Flood Basalt Province. Volcanology and Geothermal Research J 215-216: 74-82. doi: 10.1016/j.jvolgeores.2011.12.004

Whiteman KJ, Vaccaro JJ, Gonthier JB, Bauer H H (1994) The hydrogeologic framework and geochemistry of the Columbia Plateau aquifer system, Washington, Oregon and Idaho. USGS Professional Paper 1413-B. doi:10.3133/pp1413B

William JD, Everett AJ, Kenneth MK (1982) Solubility equilibria in basalt aquifers: The Columbia Plateau, eastern Washington, U.S.A. Chemical Geology 36: 15-34. doi: 10.1016/0009-2541(82)90037-7

White IC (1908) Relatório final da Comissão de Estudos das Minas de Carvão de Pedra do Brasil. Departamento Nacional de Produção Mineral. 1:1-300, 2:301-617

FIGURE CAPTIONS

Figure 1. Location map of the study area. See the geographical location in A and the geological context in B. A more detailed view in C display the limits of the area, the main outcrops, and the litostratigraphic units over the geological map (modified from CPRM, 2006).

Figure 2. Geological map showing the major lineaments identified from the satellite images 1:750,000 and 1:250,000. Rosette diagrams show the major lineaments oriented NNW, NNE, ENE and ENW and the high dispersion of orientation with the entire dataset.

Figure 3. Potenciometric, flow rate, and specific capacity maps of the wells producing from SGAS, GAS, and SGAS+GAS. A-C) Note the preferential groudwater flows indicated by blue arrows in the potenciometric maps of SGAS (A), GAS (B), and SGAS+GAS (C). In C, note the suggestion of compartments evidenced by the light green color in the nortwest, northeast, and center-south of area. D-F) Flow rate maps evidencing high values in the north and southeast and low values in the center-south, coincident with the compartment suggested in C. The highest flow rate in F) occurs associated with the discharge zone. G-I) Specific capacities maps indicating more productive potential in the northwestern and southeast areas.

Figure 4. Elevation map of the contact between sandstones of the Guarani Aquifer System (GAS) and basalts of the Serra Geral Aquifer System (SGAS) evidencing the presence of structural blocks A to F.

Figure 5. Rosette diagram showing the orientation of joints for each structural block for GAS and SGAS. Note the orientations WNW, ENE, and NE in different blocks and both aquifers.

Figure 6. Optical images of the Cantagalo well and structural data. a) Bedding surfaces (red line) and joints (pink line) in the sandstones of the Guarani Aquifer System. b) joints in the contact Guarani-Serra Geral aquifers. c) vesicular-amygdaloidal basalts with joints and a sandstone bed intercalation. In the rosette diagrams, note that NW, NE, and ENE patterns are well evident for the whole well. Near the contact Guarani-Serra Geral a NS trend is prominent.

Figure 7. Outcrops of the blocks A (A, B, E) and B (C, D, F, G). A) Basalt quarry with high degree of fracturing and columnar disjunctions. Note the principal orientation to N60-70W. B) Aeolian sandstones with a level characterized by tafoni features. Note the water percolation along the vertical

wall. C) Friable water-saturated sandstone interbedded within lava flows. D) Weathered vesicular-amygdaloidal basalt segmented by joint. E) Basalt lava flow. 1) vesicular-amygdaloidal zone; 2) horizontal disjunction; 3) vertical disjunction. F) Sandstone beds cut by a well-developed trend of N50-60W of joints. G) Volcanic rocks of the Caxias Facies with joints oriented to WNW, NW, and NE.

Figure 8. Outcrops of the blocks C (A, B, C, D) and D (C, D, F, G). A) Basalt quarry with dominance the vesicular-amygdaloidal. Note the joint orientations to NW, NNW and NE in 1) NNW and NW and NW and NE in 2). B) Cross stratification enhanced by levels of prominent iron oxide cement. Note the joint pattern orientation to WNW. C) Fractured sandstone with an evident pattern of joints to NE (yellow arrow). The sandstones are limited in the left by a basalt dyke oriented EW. D) Basalts with columnar disjunction and a fault oriented N10W crossing the vertical wall. E) N30W open joint filled by ?smectite. F) Kaolinite cement associated with cross stratifications. Rosette diagram in B) is not on the same scale as the others.

Figure 9. Outcrops of the blocks E (A, B) and F (C, D, E). A) Basalt quarry showing a well-developed vesicular-amygdaloidal, horizontal joints and water percolation (yellow arrow). Note the joint orientations to NNE. B) Sandstone near the contact with basalts. The joint pattern orientations are to NW and ENE. C) Basalt with prominent weathering features and joints oriented ENE. D) Dense joints in sandstone with orientation to WNW e NW. E) Vesicular-amygdaloidal basalt with prominent weathering overlying sandstone with joint pattern oriented to WNW and, subordinately, NE.

Figure 10. Photomicrography of sandstone thin sections. A) Moderately sorted and rounded fine-to-medium-grained sandstone with intergranular porosity and a very porous continuous conduit associated with an open joint; B) Pores isolated by the presence of cement. C) Example of non-connected intergranular pores by the obstruction by iron oxide cement. D) Incipient iron oxide cement in sandstone with 13.3% of porosity. E) Low porosity (3.0%) in quartzous sandstone. The level with coarse-grained grains represents grain flow intercalated with grain fall in aeolian dune deposits. F) Kaolinite as cement precipitated into intergranular pores. Note the light blue color of the pores indicating the presence of the cement. G) Intergranular porosity locally obstructed by iron oxide cement. H) Arkose without porosity. I) An open joint in sandstones affected by the thermal metamorphism near the contact Guarani-Serra Geral. J) Very porous sandstone derived from open intergranular space and joints.

Figure 11. Geological sections along the six structural blocks in the study area. A) Section AA' showing the elevation of the Guarani-Serra Geral contact, the water inflow positions, piezometric levels. B) Section BB'shows relationships among blocks A, C, and F. Note the intercalation of sandstones and basalts, diabase dykes, water inflows, and piezometric levels.

Figure 12. Conceptual hydrogeological model showing the altimetric variation of the contact Guarani-Serra Geral in different blocks, the preferential groundwater flow, and the porosity of sandstones associated with fractures present in both aquifers.

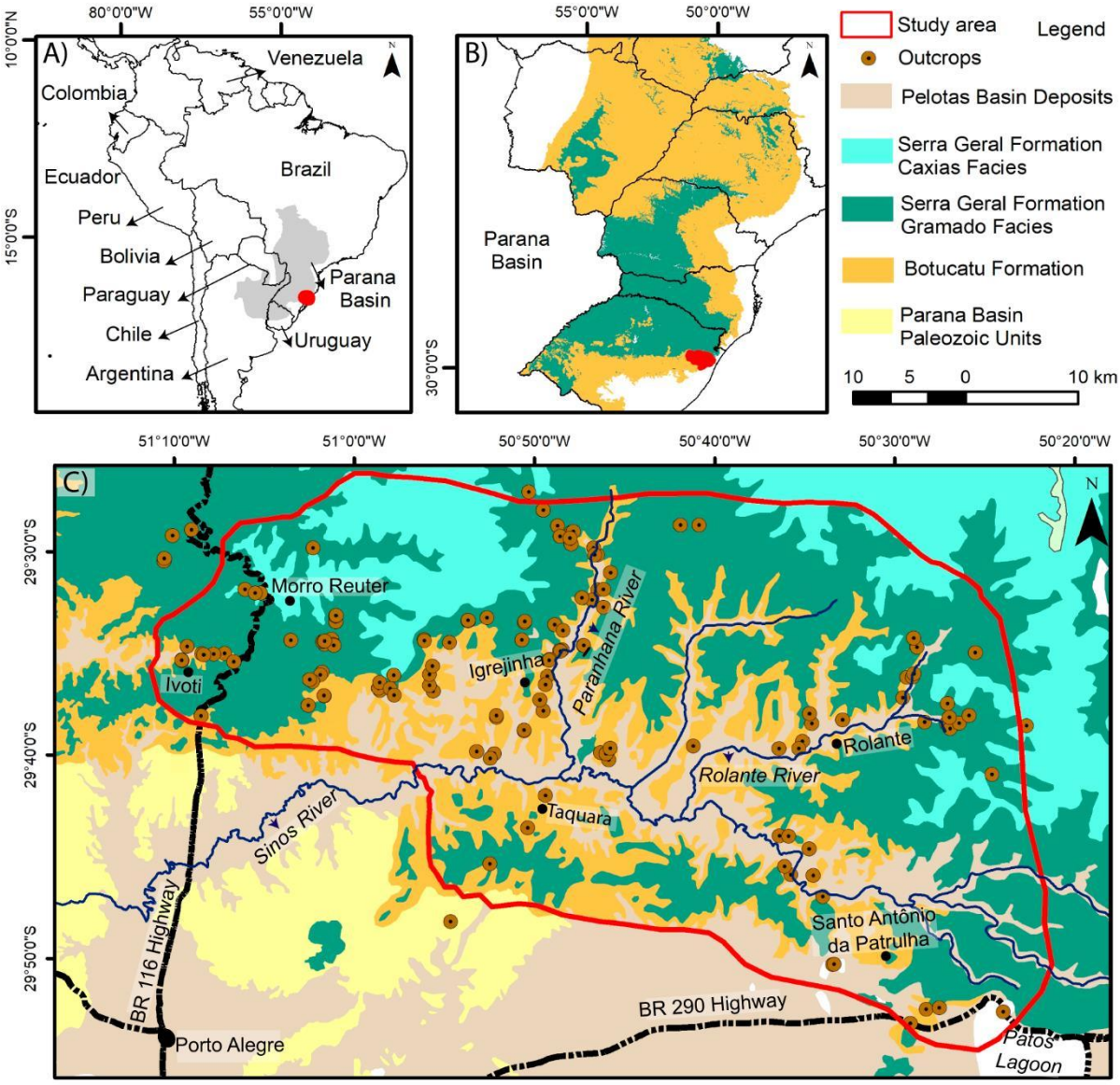
A)
B)
C)
Venezuela
Colombia
Ecuador
Brazil
Peru
Bolivia
Paraguay
Chile
Argentina
Parana Basin
Uruguay
Legend
Study area
Outcrops
Pelotas Basin Deposits
Serra Geral Formation Caxias Facies
Serra Geral Formation Gramado Facies
Botucatu Formation
Parana Basin Paleozoic Units
10 5 0 10 km
Morro Reuter
Ivoti
Igrejinha
Paranhana River
Rolante
Rolante River
Taquara
Sinos River
BR 116 Highway
Santo Antônio da Patrulha
BR 290 Highway
Porto Alegre
Patos Lagoon

Fig. 1.

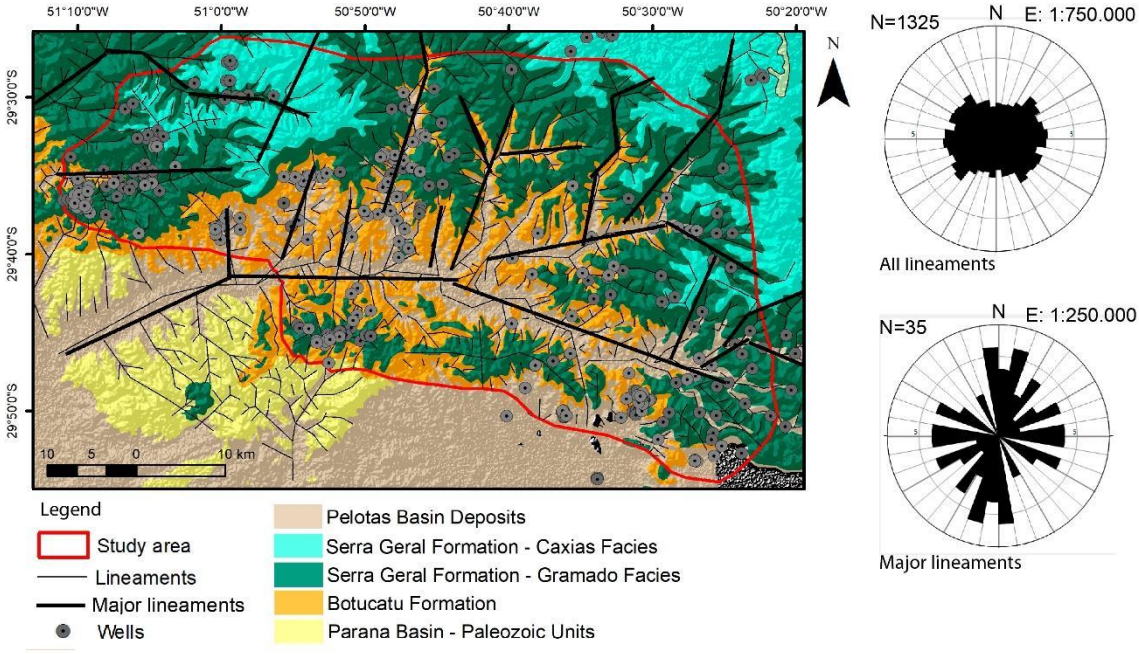
51°10'0"W
51°0'0"W
50°50'0"W
50°40'0"W
50°30'0"W
50°20'0"W
29°30'0"S
29°40'0"S
29°50'0"S
N
10 5 0 10 km
N=1325
N E: 1:750.000
All lineaments
N=35
N E: 1:250.000
Major lineaments
Legend
Study area
Lineaments
Major lineaments
Wells
Pelotas Basin Deposits
Serra Geral Formation - Caxias Facies
Serra Geral Formation - Gramado Facies
Botucatu Formation
Parana Basin - Paleozoic Units

Fig. 2.

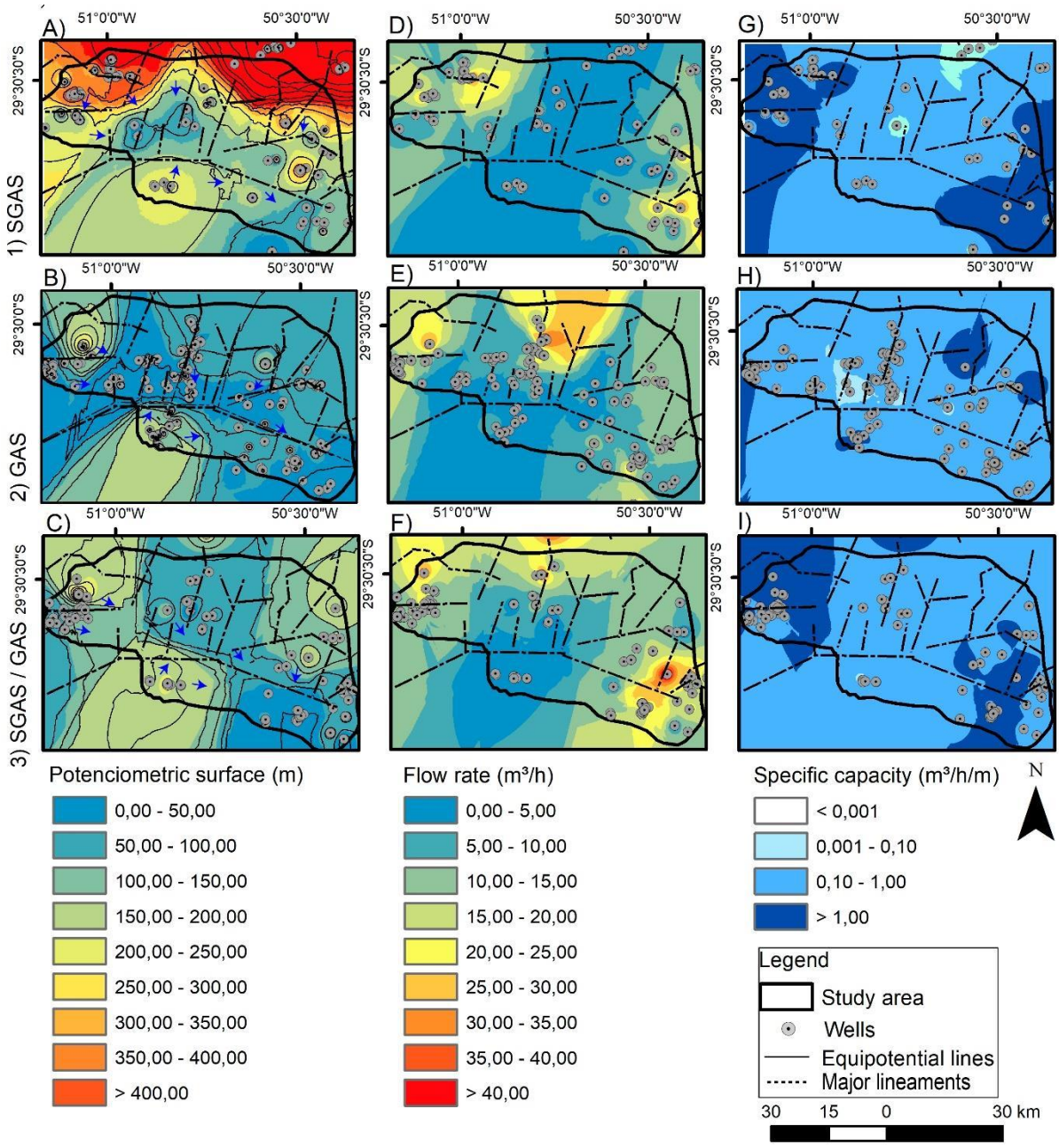
A)
D)
G)
B)
E)
H)
C)
F)
I)
51°0'0"W
50°30'0"W
29°30'0"S
29°30'30"S
1) SGAS
2) GAS
3) SGAS / GAS
Potenciometric surface (m)
0,00 - 50,00
50,00 - 100,00
100,00 - 150,00
150,00 - 200,00
200,00 - 250,00
250,00 - 300,00
300,00 - 350,00
350,00 - 400,00
> 400,00
Flow rate (m³/h)
0,00 - 5,00
5,00 - 10,00
10,00 - 15,00
15,00 - 20,00
20,00 - 25,00
25,00 - 30,00
30,00 - 35,00
35,00 - 40,00
> 40,00
Specific capacity (m³/h/m)
< 0,001
0,001 - 0,10
0,10 - 1,00
> 1,00
N
Legend
Study area
Wells
Equipotential lines
Major lineaments
30 15 0 30 km

Fig. 3.

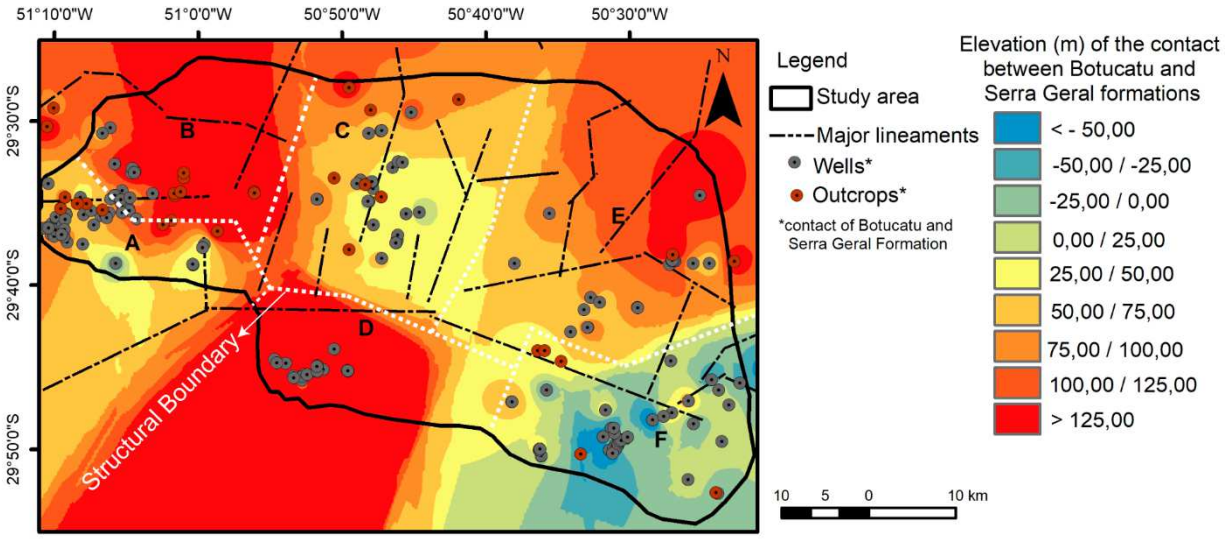
51°10'0"W
51°0'0"W
50°50'0"W
50°40'0"W
50°30'0"W
29°30'0"S
29°40'0"S
29°50'0"S
N
A
B
C
D
E
F
Structural Boundary
Legend
Study area
Major lineaments
Wells*
Outcrops*
*contact of Botucatu and Serra Geral Formation
Elevation (m) of the contact between Botucatu and Serra Geral formations
< - 50,00
-50,00 / -25,00
-25,00 / 0,00
0,00 / 25,00
25,00 / 50,00
50,00 / 75,00
75,00 / 100,00
100,00 / 125,00
> 125,00
10 5 0 10 km

Fig. 4.

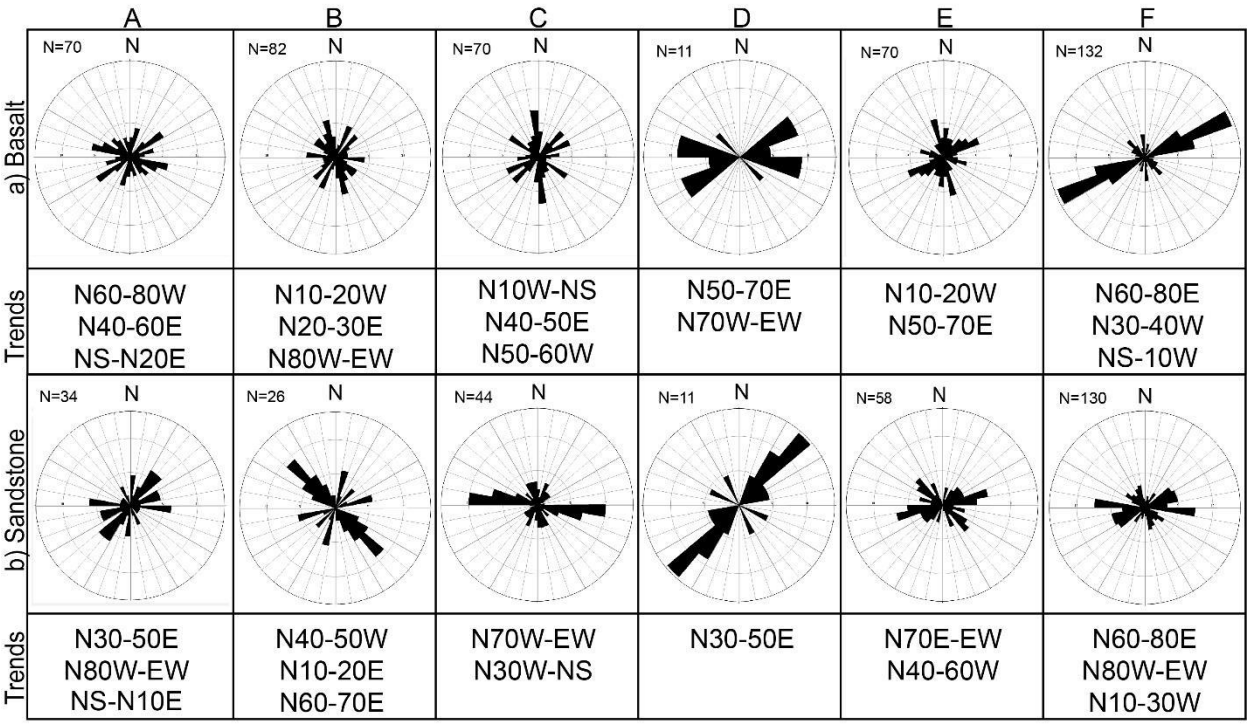
A
B
C
D
E
F
a) Basalt
N=70
N=82
N=70
N=11
N=70
N=132
Trends
N60-80W
N40-60E
NS-N20E
N10-20W
N20-30E
N80W-EW
N10W-NS
N40-50E
N50-60W
N50-70E
N70W-EW
N10-20W
N50-70E
N60-80E
N30-40W
NS-10W
b) Sandstone
N=34
N=26
N=44
N=11
N=58
N=130
Trends
N30-50E
N80W-EW
NS-N10E
N40-50W
N10-20E
N60-70E
N70W-EW
N30W-NS
N30-50E
N70E-EW
N40-60W
N60-80E
N80W-EW
N10-30W

Fig. 5.

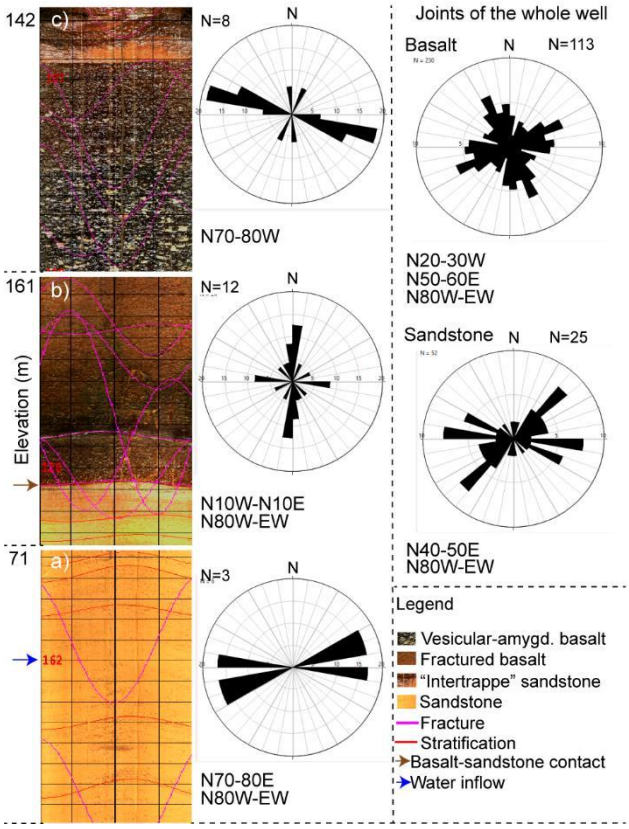
142
c)
N=8
N
N70-80W
161
b)
N=12
N
N10W-N10E
N80W-EW
Elevation (m)
71
a)
162
N=3
N
N70-80E
N80W-EW
Joints of the whole well
Basalt
N
N=113
N20-30W
N50-60E
N80W-EW
Sandstone
N
N=25
N40-50E
N80W-EW
Legend
Vesicular-amygd. basalt
Fractured basalt
"Intertrappe" sandstone
Sandstone
Fracture
Stratification
Basalt-sandstone contact
Water inflow

Fig. 6.

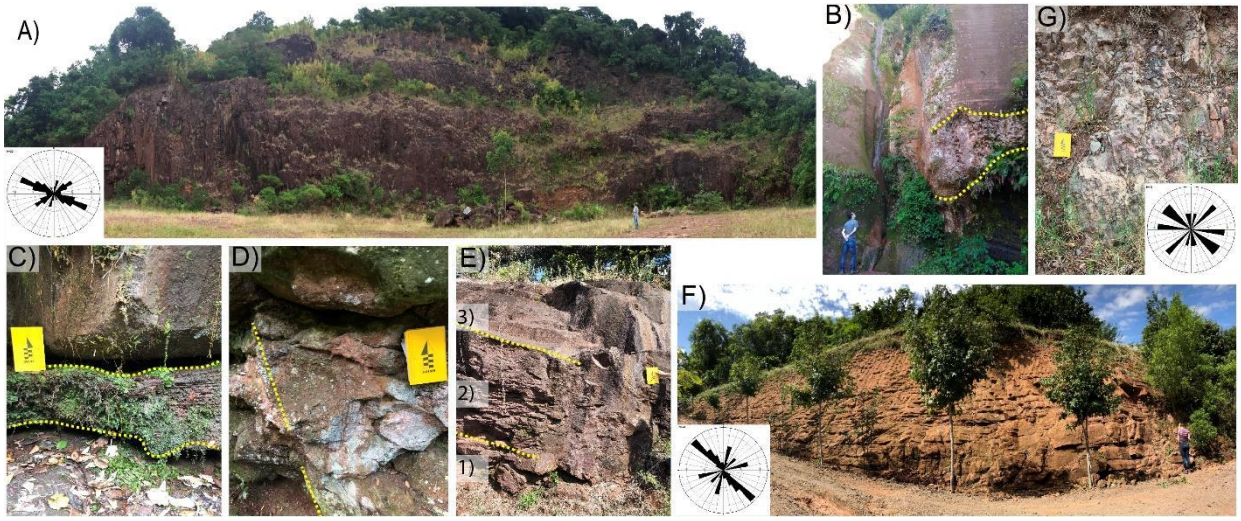

Fig. 7.

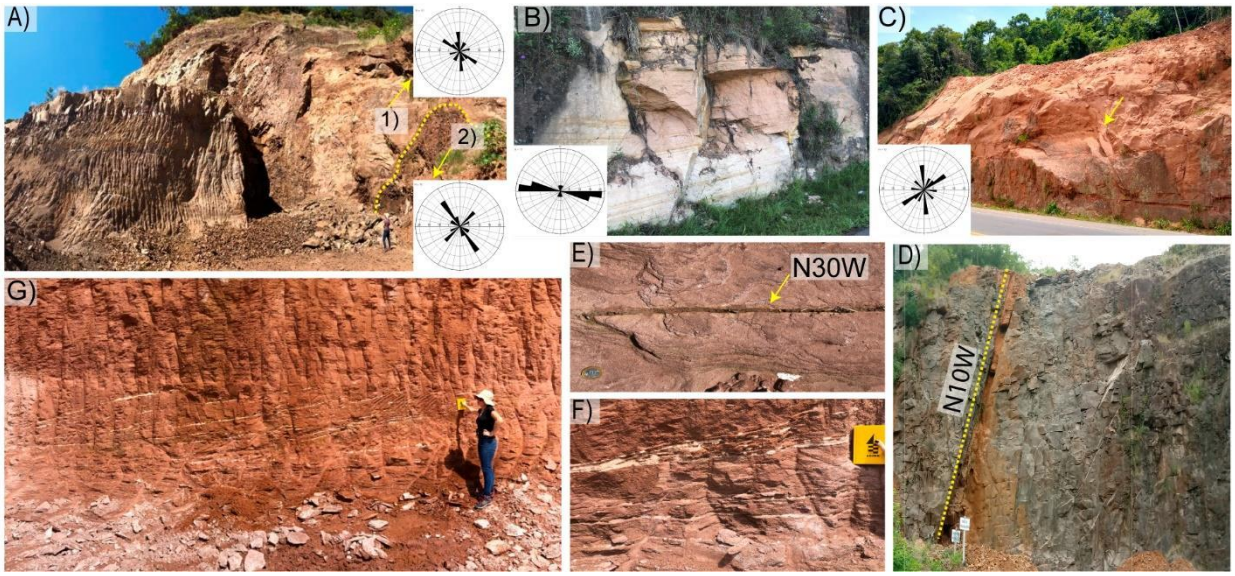

Fig. 8.

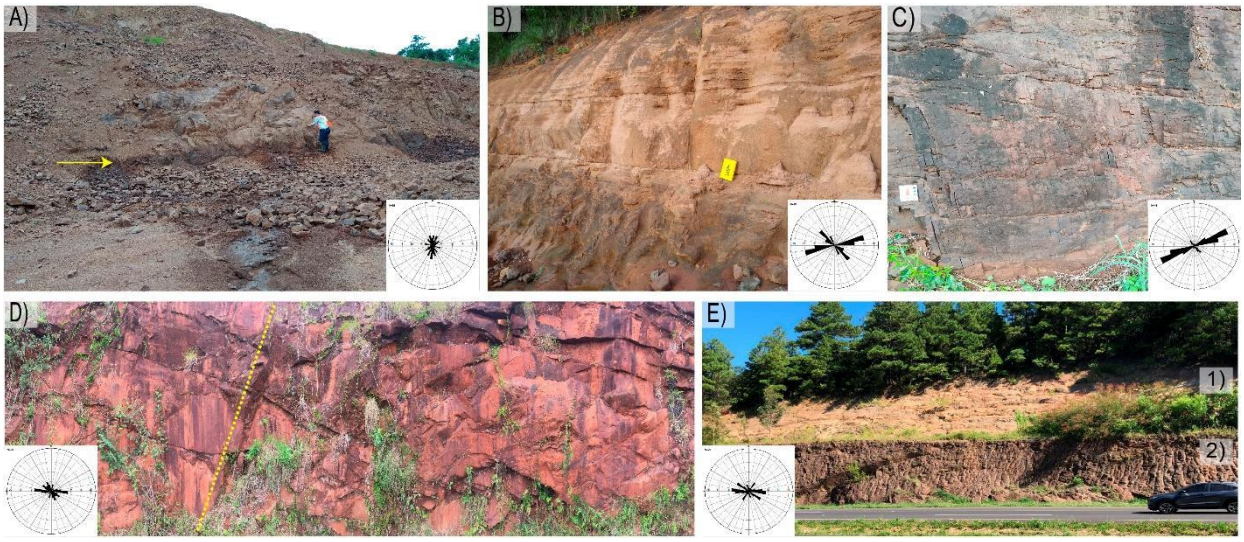

Fig. 9.

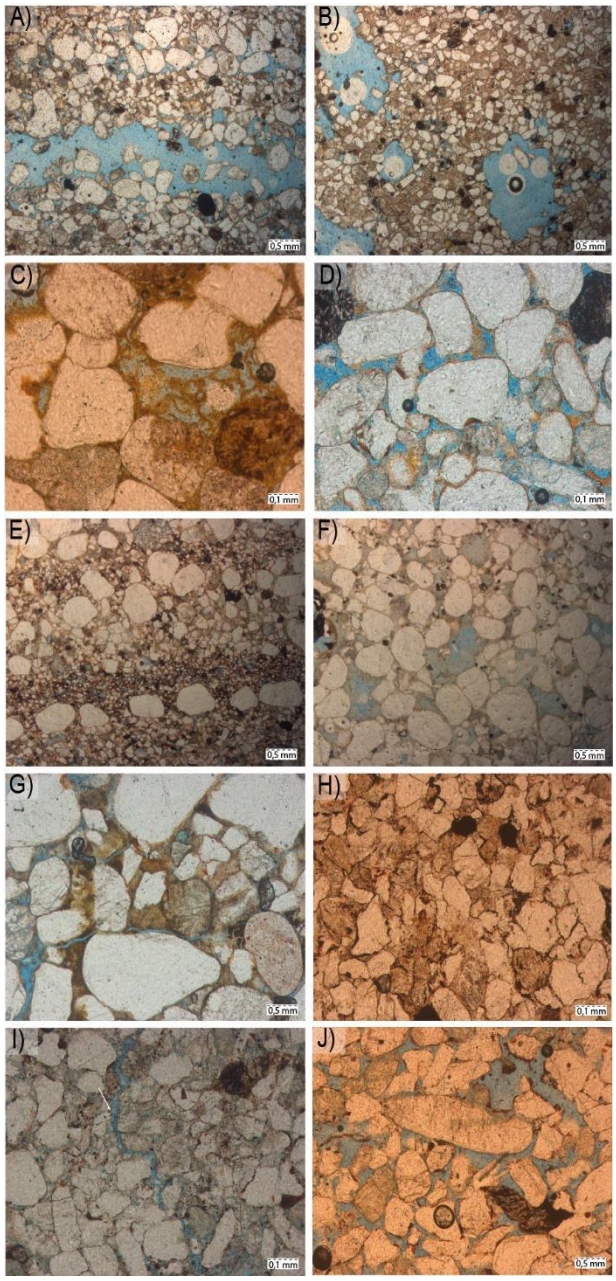
A)
0,5 mm
B)
0,5 mm
C)
0,1 mm
D)
0,1 mm
E)
0,5 mm
F)
0,5 mm
G)
0,5 mm
H)
0,1 mm
I)
0,1 mm
J)
0,5 mm

Fig. 10.

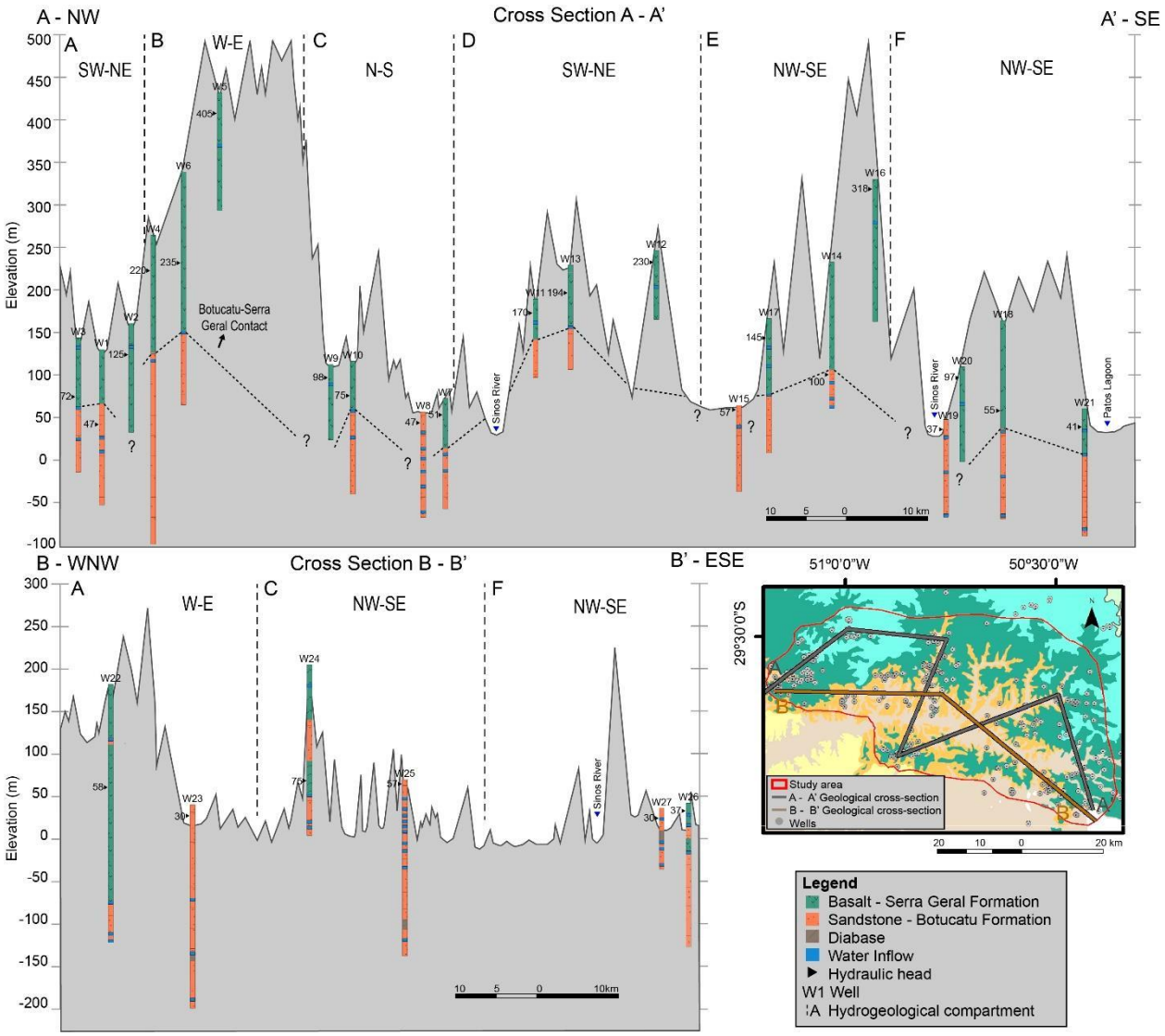
A - NW
Cross Section A - A'
A' - SE
Elevation (m)
SW-NE
W-E
N-S
SW-NE
NW-SE
NW-SE
Botucatu-Serra Geral Contact
Sinos River
Sinos River
Patos Lagoon
10 5 0 10 km
B - WNW
Cross Section B - B'
B' - ESE
W-E
NW-SE
NW-SE
Sinos River
10 5 0 10km
51°0'0"W
50°30'0"W
29°30'0"S
Study area
A - A' Geological cross-section
B - B' Geological cross-section
Wells
20 10 0 20 km
Legend
Basalt - Serra Geral Formation
Sandstone - Botucatu Formation
Diabase
Water Inflow
Hydraulic head
W1 Well
A Hydrogeological compartment

Fig. 11.

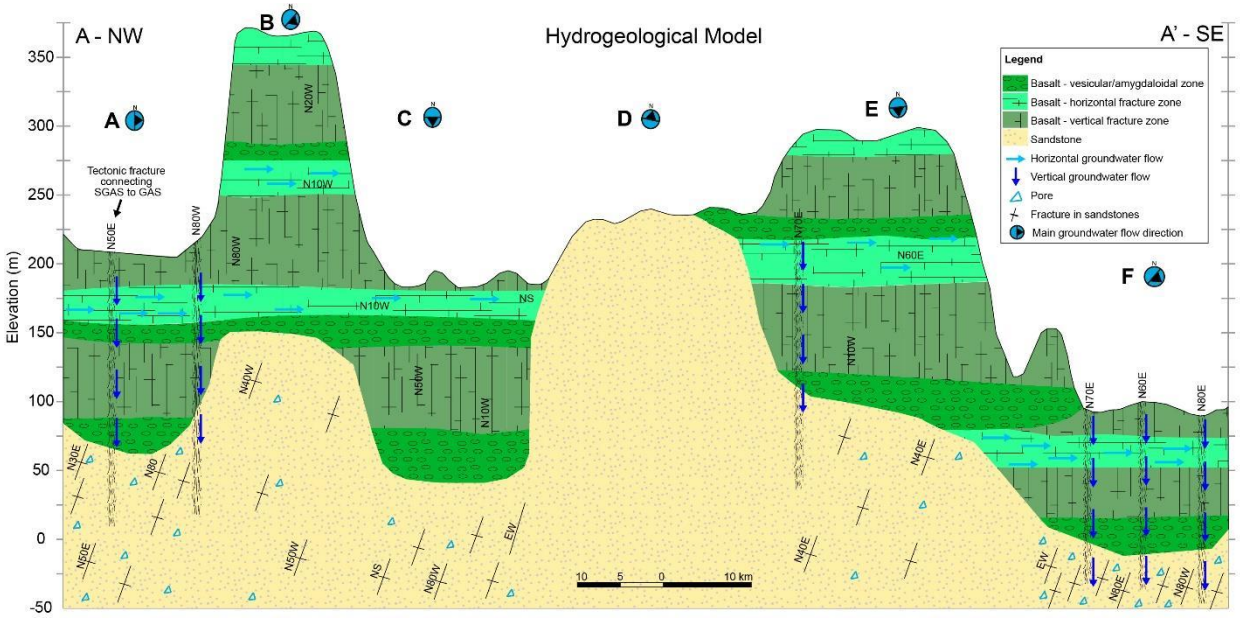
A - NW
Hydrogeological Model
A' - SE
Elevation (m)
350
300
250
200
150
100
50
0
-50
A
B
C
D
E
F
Tectonic fracture connecting SGAS to GAS
N50E
N80W
N20W
N10W
N80W
N10W
NS
N40W
N50W
N10W
N10E
N80
N60E
NS
N50W
N80W
EW
N70E
N60E
N10W
N40E
N40E
EW
N70E
N60E
N80E
N80E
N80W
10 5 0 10 km
Legend
Basalt - vesicular/amygdaloidal zone
Basalt - horizontal fracture zone
Basalt - vertical fracture zone
Sandstone
Horizontal groundwater flow
Vertical groundwater flow
Pore
Fracture in sandstones
Main groundwater flow direction

Fig. 12.

LIST OF TABLES

Table 1.

	SASG	SAG	SASG/SAG
Number of wells	99	175	101
Flow rate (m^3/h)			
Minimum	0.5	0.5	0.5
Maximum	66	44.03	60.92
Mean	10.6	10.71	14.42
Median	5.7	7.2	11.87
Standard Deviation	8.63	7.32	9.14
Specific capacity ($m^3/m/h$)			
Minimum	0.0082	0.0079	0.0054
Maximum	11.6402	5.3080	0.9975
Mean	1.2636	0.4414	0.9975
Median	0.3663	0.2086	0.2963
Standard Deviation	1.3715	0.3989	1.217

Table 2.

Block	A	B	C	D	E	F
Minimum	-27	47	-4	-33	-68	-156
Maximum	135	238	206	224	210	79
Mean	67	128	61	157	81.55	-10
Median	65	125	48	167	80.5	2
Standard Deviation	31.65	39.85	39.5	41	39.2	51

Table 3.

Block	CA	CB	CC	CD	CE	CF
Number of wells	25	5	18	10	11	30
Flow Rate (m^3/h)						
Minimum	4.06	4.55	1	1.8	1	0.5
Maximum	46.58	33	44	10.18	20.51	60.92
Mean	14.01	17.16	9.62	3.85	10.9	21.21
Median	12	15.54	6.75	2.09	12	17.22
Standard Deviation	6.56	12.57	7.26	2.56	4.42	10.72
Specific Capacity ($m^3/m/h$)						
Minimum	0.0841	0.0746	0.046	0.017	0.0117	0.053
Maximum	10	11.6105	1.14	0.25	2.85	7.21
Mean	1.2289	3.0179	0.54	0.1342	0.7574	1.0982
Median	0.356	0.1933	0.22	0.1511	0.4225	0.3769
Standard Deviation	1.302	4.2963	0.1862	0.064	0.7015	1.0261

Table 4.

Block	Thin section	Porosity	Cement (Kaolinite)	Cement (Iron Oxides)
A	113-D	7.3	25	13
A	112	17.5	19	6
B	109	8.6	38	5
C	19	2	27	10
C	23	13.3	13	2
D	116	11.8	27	5
D	118	3	31	12
D	119	1.3	44	0
E	2-B	12.5	17	3
F	7-B	1.3	9	11
F	7-C	17	15	2
F	7-D	14	10	4

Table 5.

Block	Basaltic rock predominant zone	Fracturing degree	
		Basaltic rocks	Sandstones
A	Vesciular and amygdaloidal, horizontal and vertical zones	High	Medium
B	Horizontal and vertical zones	High	Medium (few outcrops)
C	Vesciular and amygdaloidal	Medium	High
D	Null	Few or null	Few or null
E	Vesciular and amygdaloidal, horizontal and vertical zones	High	Medium
F	Vesciular and amygdaloidal, horizontal and vertical zones	High	High

6. CONSIDERAÇÕES FINAIS

Para trabalhos futuros sugere-se um aprofundamento de estudos litológicos na região, tanto das rochas basálticas quanto das areníticas. A perfilagem ótica em demais poços auxiliaria na compreensão da conexão vertical entre o SASG e SAG. Com isso, o modelo hidrogeológico conceitual poderá ser aprimorado, propiciando uma melhor visualização dos compartimentos hidrogeológicos definidos.

7. REFERÊNCIAS ADICIONAIS

Albuquerque APB (2004). Tectônica Deformadora Cenozoica na Bacia Sedimentar de Resende (Rift Continental do Sudeste do Brasil). Unpublished PhD Thesis, Universidade Federal do Rio de Janeiro, Brazil, 126 pp

Almeida FFM, Hasui Y, Brito-Neves BB, Fuck RA (1981) Brazilian Structural Provinces: an introduction. Earth Science Reviews, 17:1-29

Banks D (1992) Optimal orientation of water-supply boreholes in fractured aquifers. GroundWater, Westerville, EUA, 30(6): 895-900. doi: 10.1111/j.1745-6584.1992.tb01572.x

Banks D, Odling NE, Skarphagen H, Rohr-Torp E (1996) Permeability and stress in crystalline rocks. Terra Nova, Oxford, 8(3):223-235. doi: 10.1111/j.1365-3121.1996.tb00751.x

Banks D, Robins N (2002) An Introduction to Groundwater in Crystalline Bedrock. Norges geologiske undersokelse. Trondheim: Geological Survey of Norway, 64 pp

Bloom AL (1991) Geomorphology: a systematic analysis of late Cenozoic landforms. New Jersey: Prentice Hall, 38(3):386-387. doi: 10.1016/0033-5894(92)90047-M

Bricalli ll (2011) Padrões de lineamentos e fraturamento neotectônico no estado do Espírito Santo (sudeste do Brasil). Unpublished PhD Thesis,Universidade Federal do Rio de Janeiro, Brazil

Burbank DW, Anderson RA (2001) Tectonic Geomorphology. Oxford: Blackwell. doi: 10.1002/9781444345063

Chiang, L. C. 1984. Análise Estrutural de Lineamentos em imagens de sensoriamento remoto: aplicação ao Estado do Rio De Janeiro. Unpublished PhD Thesis, Universidade de São Paulo, Brazil, 183 pp

Coblentz DD, Richardson RM (1996) Analysis of the South American intraplate stress field, J. geophys. 100(20):245-255. doi: 10.1029/96JB00090

Coriolano ACF, Jardim de Sá EF, Cowie PA, Amaral CA (1997) Estruturas frágeis no substrato da região de João Câmara (RN): correlação com a Falha Sísmica de Samambaia. XVII Simpósio de Geologia, Resumos Expandidos: 325-329

Custodio E, Llamas M (1996) Hidrología Subterránea. 2. ed. Barcelona: Omega,

Feitosa FAC, Manoel Filho J (2000) Hidrogeologia: conceitos e aplicações. CPRM/LABHID-UFPE, Fortaleza, 391 pp.

Feitosa FAC, Manoel Filho J, Feitosa EC, Demetrio JGA (2008) Serviço Geológico do Brasil - CPRM. Hidrogeologia: conceitos e aplicações. CPRM: LABHID, Rio de Janeiro, 812 pp

Fernandes AJ, Rudolph D (2011) The influence of Cenozoic Tectonics on the groundwater-production capacity of fractured zones: a case study in Sao Paulo, Brazil. Hydrogeol J. 9(2):151-167. doi:10.1007/s100400000103

Foster S, Ventura M, Hirata R (1993) Poluição das águas subterrâneas: um documento executive da situação da América Latina e Caribe com relação ao abastecimento de água potável. Instituo Geológico (Séries Manuais), São Paulo, 55 pp

Freeze RA, Cherry JA (1979) Groundwater. New Jersey: Prentice Hall, 604 pp. doi: 10.1177/030913338100500412

Giardin AE, Faccini UF (2002) Heterogeneidades faciológicas e hidroestratigrafia do Aqüífero Guarani na região central do Rio Grande do Sul: abordagem metodológica e resultados preliminares. In: Congresso Brasileiro de Águas Subterrâneas, 12, Florianópolis, Anais, 16 pp

Guidicini G, Campos JO (1968) Notas sobre a morfogênese dos derrames basálticos. Boletim da Sociedade Brasileira de Geologia, São Paulo, 17(1):28pp

Gomes MEB (1996) Mecanismos de resfriamento, estruturação e processos pós-magmáticos em basaltos da Bacia do Paraná - Região de Frederico Westphalen (RS), Brasil. Unpublished PhD Thesis, Universidade Federal do Rio Grande do Sul, Brazil, 271 pp

Hasui Y (1990) Neotectônica e aspectos fundamentais da tectônica ressurgente no Brasil.In: SBG/MG, Workshop Sobre Neotectônica e Sedimentação Cenozóica Continental no Sudeste Brasileiro. Boletim SBG/MG, Belo Horizonte, Anais, 11:11-31.

Menezes MRF, Jardim De Sá EF (1999) Caracterização do faturamento neotectônico em rochas cristalinas: o exemplo da Grota da Fervedeira, Santana do Matos, RN. VII Simpósio Nacional de Estudos Tectônicos, Lençóis, Bol. Res. Exp.: 62-66.

Neves MA (2005) Análise integrada aplicada à exploração de água subterrânea na Bacia do Rio Jundiaí (SP). Unpublished PhD Thesis, Universidade Estadual Paulista, Brazil, 200 pp

Obruchev VA (1948) Osnovnye cherty kinetiki i plastiki neotektoniki. Akad. Nauk. SSSR Izv. Serv. Geol., 5: 13-24

Odling NP (1993) An investigation into the permeability of a 2D natural fracture pattern. Memories VVIV Congress International Asociation Hydrogeologist, Oslo, 291-300

O'leary IW, Friedman JD, Pohn HA (1976) Lineaments, linear, lineation: some proposed new standarts for old terms. Geology Society of America Bulletin, 87:1463-1469. doi: 10.1130/0016-7606(1976)87<1463:LLLSPN>2.0.CO;2

Rebouças Ac; Braga B; Tundisi JG (2006) Águas Doces no Brasil, 3° ed. São Paulo: Escrituras.

Riccomini C (1989) O rift continental do sudeste do Brasil. Unpublished PhD Thesis, Universidade de São Paulo, 319 pp

Saadi A (1993) Neotectônica da plataforma brasileira: esboço e interpretação preliminares. Geonomos, 1(1):1-15. doi: 10.18285/geonomos.v1i1e2.233

Salvador ED (1994) Análise neotectônica da região do vale do rio Paraíba do Sul compreendida entre Cruzeiro (SP) e Itatiaia (RJ). Unpublished PhD Thesis, Universidade São Paulo, 174 pp

Salvador ED, Riccomini C (1995) Neotectônica da região do alto estrutural de Queluz (SP-RJ, Brasil). Revista Brasileira de Geociências, 2(3):151-164

Sibson RH (1994) Crustal stress, faulting and fluid flow. In: Parnell, J, (Ed.) Geofluids: origin, migration and evolution of fluids in sedimentary basins. Geological Society Special Publication, 78: 69-84. doi: 10.1144/GSL.SP.1994.078.01.07

Silva TP (2006) Neotectônica na região da Zona de Cisalhamento do rio Paraíba do Sul e areas adjacentes. Unpublished PhD Thesis, Universidade Federal do Rio de Janeiro, Brazil, 2006, 125 pp

Snow DT (1969) Anisotropic permeability of fractured media. Water Resources Research, Washington, 5(6):1273-189. doi: 10.1029/WR005i006p01273

Stewart Is, Hancock PL (1994) Neotectonics. In: HANCOCK PL (Ed.) Continental Deformation. Pergamon Press, 370-409

Strieder AK, Amaro VE (1997) Estruturas de lineamentos extraídos de imagens de sensores remotos. EGATEA. Revista Escola de Engenharia, Porto Alegre, 25:109-117

Summerfield MA (1986) Tectonic Geomorphology: macroscale perspectives. Progress in Physical Geography, 10(2):227-238. doi: 10.1177/030913338701100305